tween the applied field ($H\cdot S$) and the ratio of the transverse magnetoresistance to the longitudinal magnetoresistance ($\Delta R\perp/\Delta R_{11}$). In this relationship $\Delta R\perp/\Delta R_{11}=A+B(H\cdot S)$, changes in $O_2$ doping and work hardening had little effect on the zero field intercept $A$ which remained relatively constant about $\Delta R\perp/\Delta R_{11}\sim 2$. The slope ($B$) is also independent of work hardening, but decreases with $O_2$ doping and reaches a minimum value for the conditions of Curve III. This decrease can be inferred from Fig. 1, since the Kohler plot of the transverse magnetoresistance is the same for all samples.

Thus, the longitudinal magnetoresistance of copper, as well as the low-temperature conductivity, is sensitive to the presence of impurity induced effects and due regard for their possible presence must be given in any interpretation of data. For polycrystalline copper, the saturation value of the longitudinal magnetoresistance for the pure metal appears to lie between $1>\Delta R_{11}/R_{4.2°K}>0$.

PHYSICAL REVIEW VOLUME 119, NUMBER 5 SEPTEMBER 1, 1960

# Cascade Capture of Electrons in Solids

MELVIN LAX
*Bell Telephone Laboratories, Murray Hill, New Jersey*
(Received April 21, 1960)

Enormous capture cross sections in the range $10^{-15}$ cm$^2$ to $10^{-12}$ cm$^2$ have been observed for a wide variety of Coulomb attractive centers in Si and Ge, some involving binding energies many times the Debye energy. Whereas multiphonon transitions to the ground state yield cross sections five to ten orders of magnitude too small, capture into excited states of large radius followed by a cascade of one-phonon transitions leads to cross sections of the right order of magnitude. The initial capturing event is likely to involve an optical phonon or an intervalley collision in the room temperature range, but the acoustic phonon contribution will predominate at low temperatures.

Subsequent collisions may eject the electron or cause it to increase its binding energy. The "sticking probability," or probability of eventual capture into the ground state, becomes significant for binding energies of order $kT$. As the temperature is reduced capture into orbits of larger radius becomes effective, and, at least for the acoustic phonon case the cross section increases rapidly with decreasing temperature, and with decreasing electron energy. The large cross sections $10^{-17}$ cm$^2$ to $10^{-15}$ cm$^2$ found for neutral centers can be explained on a similar basis, the attractive potential in this case being provided by the large polarizability of the neutral center.

## 1. INTRODUCTION[1]

### Traps and Recombination Centers

THE pioneer work of Shockley and Read[2] and Hall[3] suggested that the recombination of electrons and holes in solids could best be understood in terms of the successive capture of an electron and hole at a localized site ("recombination center") in the crystal. Indeed Burton, Hall, Morin, and Severiens[4] showed that Cu and Ni impurities in germanium behaved as recombination centers at room temperature, whereas Shulman and Wyluda[5] showed that at lower temperatures Cu behaves as a trap.

The distinction between a trap and a recombination center is therefore a quantitative rather than a qualitative one. For the sake of definiteness we shall adopt the following picture: A minority carrier is captured at a center. If the carrier lives a mean lifetime in the captured state and is ejected (e.g., thermally), we may regard the center as a trap. If, however, before thermal ejection can occur, a majority carrier is trapped, recombination will have taken place, and the center may be regarded as a recombination center. Which role a center will play depends then on the concentration of majority carriers and on the relative cross section for capture of minority and majority carriers.

Perhaps the simplest picture to adopt is as follows: Centers that are singly charged and attractive to minority carriers are likely to act as recombination centers since the cross section for the subsequent neutral capture of a majority carrier may only be one order of magnitude lower than the minority carrier cross section, but the number of majority carriers may be sufficiently large that recombination will occur before ejection. Centers that are doubly charged and attractive to minority carriers are likely to act as traps. They will possess a large cross section for the minority carrier, but after capture will be repulsive to the majority carrier. The repulsion can reduce the cross section by many orders of magnitude so that ejection of the trapped minority carrier will be much more likely than recombination.

[1] A detailed summary of the results contained in this paper was presented by M. Lax at the *Proceedings of the International Conference on Semiconductors, Rochester, 1958* [J. Phys. Chem. Solids **8**, 66 (1959)]. Our choice of mechanism and partial results were presented to the American Physical Society: M. Lax, Bull. Am. Phys. Soc. **1**, 128 (1956); **2**, 147 (1957).
[2] W. Shockley and W. T. Read, Phys. Rev. **87**, 835 (1952).
[3] R. N. Hall, Phys. Rev. **87**, 387 (1952).
[4] J. A. Burton, G. W. Hall, F. J. Morin, and J. C. Severiens, J. Phys. Chem. **57**, 853 (1953).
[5] R. G. Shulman and B. J. Wyluda, Phys. Rev. **102**, 1455 (1956).

## Cross Sections and Rates

In an experiment, one does not observe directly the capture cross section, but rather a capture rate constant $B$ cm$^3$/sec that describes the rate at which electrons leave the conduction band via the equation

$$dn/dt = -BnN, \tag{1.1}$$

where $n$ is the density of electrons, and $N$ is the number of empty traps. If all the electrons had the same energy $E_0$, the rate constant would be related to the cross section by a factor of the velocity

$$B(E_0) = v_0\sigma(E_0); \quad v_0 = (2E_0/m)^{\frac{1}{2}}. \tag{1.2}$$

The experimental constant $B$ is an average over $B(E_0)$ taking into account the *actual* electron energy distribution. For the usual case in which a thermal equilibrium distribution is present, we may write

$$B = \langle v_0\rangle\sigma = (4kT/m\pi)^{\frac{1}{2}}\sigma, \tag{1.3}$$

where

$$\sigma = \langle v_0\sigma(E_0)\rangle/\langle v_0\rangle,$$

or

$$\sigma = \int E_0\sigma(E_0)\exp(-E_0/kT)dE_0 \Big/ \int E_0\exp(-E_0/kT)dE_0. \tag{1.4}$$

In Eq. (1.4) two factors of $E_0^{\frac{1}{2}}$, one from $v_0$ and one from the Boltzmann distribution, give rise to the factor $E_0$.

The cross section most frequently quoted in experimental papers is obtained by dividing the observed rate by the root mean square velocity:

$$\sigma_{\rm rms} = B/(3kT/m)^{\frac{1}{2}}. \tag{1.5}$$

The rms cross section may be computed from ours by

$$\sigma_{\rm rms} = (4/3\pi)^{\frac{1}{2}}\sigma, \tag{1.6}$$

where $\sigma$ will be computed in our paper from Eq. (1.4).

In spite of the slight arbitrariness in defining a cross section (which is unimportant when our chief aim is to predict the correct order of magnitude) it is convenient to quote cross sections since they convey an impression of the effective size of a capturing center.

## Experimental Results

An adequate survey of the experimental work on trapping and recombination cross sections is beyond the scope of the present paper. A survey of early work through 1954 has been given by Rose,[6] and more recent work has been reviewed by Bemski.[7] Table I summarizes cross sections on some centers of presumably known charge. Additional experimental data can be found in the proceedings of the 1958 Semiconductor Conference.[8]

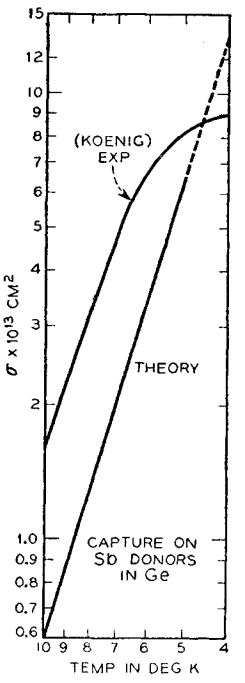


FIG. 1. The cascade theory, with acoustic phonons as the mechanism, is compared with experimental results of S. Koenig for capture of electrons on Sb donors in germanium. The theoretical curve (without a cutoff for the finite density of donors) is computed by means of

$$\sigma \approx (4^5/6)(\sigma_1/\gamma^4)[\ln(\gamma/1.781\delta) + (\delta/\gamma)],$$

and

$$\sigma_1 = (\pi/12)(Ze^2/\kappa\tfrac{1}{2}mc^2)^3(l_c)^{-1} \approx 7\times10^{-9}\ \text{cm}^2,$$

using Fig. 6 to interpolate for $\delta$. We have used $\kappa=12$, $m=\frac{1}{4}m_0$, $c=4\times10^5$ cm/sec and $l_c\gamma\simeq1.84\times10^{-2}$ independent of temperature, based on a room temperature mean free path of $8\times10^{-6}$ cm and a room temperature $\gamma=kT/\frac{1}{2}mc^2=2300$.

Cross sections have been observed which are exceedingly small—in the range $10^{-24}$ cm$^2$ to $10^{-21}$ cm$^2$ for centers which are known or presumed to be repulsive. (See for example $Mn^-$ in Table I.) Cross sections so large, from $10^{-15}$ cm$^2$ to $10^{-12}$ cm$^2$, that we have dubbed them "giant traps," have been observed for centers known or presumed to possess a Coulomb attractive charge.[9–11] (See Fig. 1.) [Bemski's cross sections (Table I) for singly charged attractive Au centers in Si of $10^{-15}$ cm$^2$ suggest that the traps observed by Haynes and Hornbeck[12] in Si with room temperature cross sections of $10^{-13}$ cm$^2$ are doubly or triply charged.[13]]

Centers that are known or presumed to be neutral are usually found to have large cross sections in the range $10^{-17}$ cm$^2$ to $10^{-15}$ cm$^2$ which are relatively insensitive to temperature. [Some Cu cross sections which appear to have a temperature dependence characterized by an activation energy[5,14] have been more simply explained by Kalashnikov[15] by taking into account the multilevel nature of the Cu center

[6] For a review of experimental work through 1954, see Albert Rose, Phys. Rev. **97**, 322 (1955); RCA Rev. **12**, 362 (1951).
[7] G. Bemski, Proc. Inst. Radio Engrs. **46**, 990 (1958).
[8] *Proceedings of the International Conference on Semiconductors, Rochester, 1958* [J. Phys. Chem. Solids **8**, 52–86 (1959)].
[9] S. Koenig, J. Phys. Chem. Solids **8**, 227 (1959).
[10] S. Koenig, Phys. Rev. **110**, 986, 988 (1958).
[11] S. Koenig, *International Conference on Solid-State Physics in Electronics and Telecommunications, Brussels, June, 1958* (Academic Press, New York, 1960).
[12] J. A. Hornbeck and J. R. Haynes, Phys. Rev. **97**, 311 (1955); **100**, 606 (1955).
[13] Evidence that Cu and Au may act as triple acceptors in germanium has been presented by H. H. Woodbury and W. W. Tyler, Phys. Rev. **105**, 84 (1957).
[14] J. F. Battey and R. M. Baum, Phys. Rev. **100**, 1634 (1955).
[15] S. G. Kalashnikov, J. Phys. Chem. Solids **8**, 52 (1959).

TABLE I. Capture cross sections (in units of $10^{-16}$ cm$^2$) and their temperature dependence (the exponent $n$ in $T^{-n}$ is shown in the last column).

| Host | Center | $T$ | $\sigma_n^{(+)}$ | $\sigma_n^{(0)}$ | $\sigma_n^{(-)}$ | $\sigma_p^{(0)}$ | $\sigma_p^{(-)}$ | $\sigma_p^{(=)}$ | $\sigma_p^{(\equiv)}$ | Exponent | First author |
|---|---|---|---|---|---|---|---|---|---|---|---|
| Ge | Sb | 4° | $10^4$ | | | | | | | 2.7 | Koenig[a] |
| | Fe | 300° | 10 | | | | | | | | Glinchuk[b] |
| | | 300° | | 1–10 | | | | | | | Tyler[c] |
| | | 300° | | | | | 30 | 100 | | | Glinchuk[d] |
| | Co | 300° | | 1–10 | | | | | | | Glinchuk[d] |
| | | 300° | | 10 | | | | | | | Glinchuk[b] |
| | Ni | 300° | | | 0.8 | | | >40 | | | Burton[e] |
| | | 300° | | 20 | 3 | | | 200 | | | Kalashnikov[f] |
| | | 300° | | 1 | 6 | | | 100 | | | Wertheim[g] |
| | | 77° | | | | | 1000 | | | | Newman[h] |
| | Cu | 300° | | | 0.1 | | | 1 | | | Burton[e] |
| | | 300° | | | 0.15 | 0.3 | | 1 | 2 | | Mashovets[i] |
| | | 20° | | | | | 500 | | | | Brown[j] |
| | | 300° | | 1.5 | 0.15 | | | 0.4 | 1 | $2(\sigma_n^{(-)})$ | Kalashnikov[k] |
| | Mn | 300° | | >30 | | | | | | | Newman[h] |
| | | 150° | | | $<10^{-4}$ | | | | | | Newman[h] |
| | Ag | 300° | | | 1 | | | | | | Glinchuk[l] |
| | Au | 300° | | | 2 | | | 100 | | | Glinchuk[l] |
| | Bi | 300° | | | | 10 | | | | | Alekseyeva[m] |
| | Sb | 300° | | | | <0.01 | | | | | Alekseyeva[m] |
| | Tl | 300° | | 10 | | | | | | | Alekseyeva[m] |
| | Ga | 300° | | <0.01 | | | | | | | Alekseyeva[m] |
| | Zn | 300° | | <0.0004 | | | | | | | Kalashnikov[n] |
| Si | Au | 300° | 35 | | | | | | | 2.5 | Bemski[o] |
| | | 300° | | | | | 10 | | | 4 | Bemski[o] |
| | | 300° | | 5 | | >3 | | | | $0(\sigma_n^{(0)})$ | Bemski[o] |
| | | 77° | 1000 | 20 | | 20 | 3000 | | | | Davis[p] |
| | In | 100° | | | | | 1500 | | | 2 | Wertheim[q] |
| | | 100° | | 1.1 | | | | | | 1 | Wertheim[q] |

[a] S. Koenig, J. Phys. Chem. Solids **8**, 227 (1959); Phys. Rev. **110**, 986, 988 (1958).
[b] K. D. Glinchuk, E. G. Miseliuk, and N. N. Fortunatova, Ukraïn. Fiz. Zhur. **4**, 207 (1959).
[c] W. W. Tyler and H. H. Woodbury, Bull. Am. Phys. Soc. **1**, 127 (1956).
[d] K. D. Glinchuk, E. G. Miseliuk, and N. N. Fortunatova, Zhur. Tekh. Fiz. (U.S.S.R.) **27**, 2451 (1957) [translation: Soviet Phys. (Tech. Phys.) **2**, 2283 (1957)].
[e] J. Burton, R. Hull, F. Morin, and J. Severiens, J. Phys. Chem. **57**, 853 (2953). Charges on Ni could be one unit more positive than shown in this table.
[f] S. G. Kalashnikov and K. P. Tissen, Fiz. Tverdago Tela **1**, 1754 (1959); **1**, 545 (1959) [translation: Soviet Phys.—Solid-State Phys. **1**, 1604 (1959); **1**, 491 (1959)].
[g] G. K. Wertheim, Phys. Rev. **115**, 37 (1959).
[h] R. Newman and W. W. Tyler, in *Advances in Solid-State Physics*, edited by F. Seitz and D. Turnbull (Academic Press, New York, 1959), Vol. 8, p. 49.
[i] T. V. Mashovets, Zhur. Tekh. Fiz. (U.S.S.R.) **28**, 1140 (1958) [translation: Soviet Phys. (Tech. Phys.) **28**, 1062 (1958)].
[j] D. A. H. Brown, J. Electronics and Control **4**, 341 (1958).
[k] S. G. Kalashnikov, J. Phys. Chem. Solids **8**, 52 (1959); N. G. Zhdanova, S. G. Kalashnikov, and A. I. Morozov, Fiz. Tverdago Tela **1**, 535 (1959) [translation: Soviet Phys.—Solid-State Phys. **1**, 481 (1959)]; S. G. Kalashnikov and A. I. Morozov, Fiz. Tverdago Tela **1**, 1294 (1959) [translation: Soviet Phys.—Solid-State Phys. **1**, 1182 (1959)]. See also K. Konstantinesku, Fiz. Tverdago Tela **1**, 1766 (1959) [translation: Soviet Phys.—Solid-State Phys. **1**, 1616 (1959)].
[l] K. D. Glinchuk, E. G. Miseliuk, and N. N. Fortunatova, Fiz. Tverdago Tela **1**, 1345 (1959) [translation: Soviet Phys.—Solid-State Phys. **1**, 1234 (1959)].
[m] V. G. Alekseyeva, S. G. Kalashnikov, L. P. Kalnach, I. V. Karpova, and A. J. Morozov, Zhur. Tekh. Fiz. (U.S.S.R.) **27**, 1931 (1957) [translation: Soviet Phys. (Tech. Phys.) **2**, 1794 (1957)].
[n] S. G. Kalashnikov, E. Iu. Lvova, and V. V. Ostroborodova, J. Tech. Phys. (U.S.S.R.) **27**, 1925 (1957) [translation: Soviet Phys.(Tech. Phys.) **2**, 1789 (1958)].
[o] G. Bemski, Phys. Rev. **111**, 1515 (1958).
[p] W. D. Davis, Phys. Rev. **114**, 1006 (1959).
[q] G. K. Wertheim, Phys. Rev. **109**, 1086 (1958).

using the statistics of Sah and Shockley.[16] A similar situation seems to prevail[17] for Ni.]

The work of Bemski and Davis on Au in Si and of Koenig[9–11] on Sb in Ge (see Table I and Fig. 1) indicate that the capture cross sections for Coulomb attractive centers increase rapidly with decreasing temperature as $T^{-n}$ with $n$ as large as 4.

## Explanation of the Data: The Cascade Hypothesis

We propose to explain this enormous range of experimental data as follows: The geometrical size of a center $10^{-16}$ cm$^2$ is not an adequate estimate for cross sections because the electron must not only come to the vicinity of the center it must also perform the unlikely event of losing perhaps 0.5 ev of energy. The conveyance of such energy to phonons might require the production of ten or twenty phonons. A direct transition to the ground state of a trap involving such a multiphonon process is likely to have an exceedingly small cross section,[18,19] say $10^{-22}$ cm$^2$ in a semiconductor where the electron-phonon interaction is weak. For repulsive centers, which possess no excited states, this is the only process available (aside from optical and Auger processes which are also weak) and we therefore expect such exceedingly small cross sections.

Centers with a long-range Coulomb attractive po-

[16] Chin-Tang Sah and W. Shockley, Phys. Rev. **109**, 1103 (1958).
[17] G. K. Wertheim, Phys. Rev. **115**, 37 (1959); J. Okada, J. Phys. Soc. Japan **12**, 741, 1338 (1957).
[18] H. Gummel and M. Lax, Ann. Phys. **2**, 28 (1957).
[19] For a review of earlier theoretical work see M. Lax, *Proceedings of the Conference on Photoconductivity, Atlantic City, November 4–6, 1954*, edited by R. G. Breckenridge *et al.* (John Wiley & Sons, Inc., New York, 1956), pp. 111–145.

tential possess a series of excited states whose radius increases without bound. The states of large radius explain the large observed capture cross section. Indeed, the total cross section for capture into all excited states would diverge. Roughly speaking, however, one must include only states whose binding energy is greater than $kT$. Lowering the temperature then permits contributions from states of increasing radius. Thus we explain the rapid increase of observed cross sections with decreasing temperature (see Fig. 1).

We assume that in the vicinity of binding energy $kT$ there are states closely enough spaced for one-phonon transitions to be possible. As a result of these transitions the electron escapes, or moves closer to the ground state. The last step, from a first excited state to the ground state may require a multiphonon transition, or the emission of radiation. This last step is undoubtedly the step limiting the rate at which electrons enter the ground state of the trap. But the cross section, as measured by the rate at which electrons leave the conduction band, is not limited nor even affected by the rate of this last step[20] (providing the ionization energy of the first excited state is large compared to $kT$): electrons caught in excited states are unavailable for conduction.

For neutral centers, we suggest that a quasi-long range interaction (an inverse fourth-power potential) is provided by the polarizability of the center. (Traps in solids are significantly more polarizable than free atoms because of their lower ionization energies.) Since the radius at which the potential energy is $kT$ now varies as $T^{\frac{1}{4}}$, we expect a much less temperature dependent cross section. Since the contributions come from smaller radii than for the Coulomb attractive case, the resulting cross section is much more sensitive to the details of the potential at shorter ranges, i.e., the chemical nature of the trapping center.

## Classical Approximations

A calculation of the sum of the cross sections for capture into all of the excited states of a center would, indeed, be a laborious task. When highly excited states are important, however, we anticipate from the Bohr correspondence principle that a classical calculation will be valid, i.e., that the motion of the electron between collisions can be described by a classical orbit. The probability per unit time that a collision will take place can be computed at each point of the orbit by treating the electron as if it were a plane wave with the energy and momentum appropriate to that point of the orbit. This procedure is equivalent to neglecting the accelerating effect of the attractive field during the collision and is valid if the fractional energy change along the orbit is small over a time of the order of the "duration of the collision."

## Mechanisms for Energy Loss

In order to be captured the electron must lose enough energy in a collision to go into a bound orbit. The energy can be carried away by: (1) a photon, (2) another electron or hole, (3) optical phonons, (4) acoustical phonons: (1) cross sections for radiative capture can be readily calculated from first principles, or by scaling similar calculations for proton-electron recombination. The resulting cross sections are a few orders of magnitude too low to explain observed results. (2) Auger recombination with the help of another carrier will in general lead to nonexponential decay, or in steady-state experiments to a concentration dependence of the lifetime that is not usually observed.[21] Of course Auger recombination should occur when high carrier densities are present.[22] (3) Optical phonons are generally not very effective in nonionic materials in producing the momentum transfers required to produce resistivity. However, each optical phonon collision transfers so much more energy to the lattice than an acoustical phonon per collision that the Joulean heat loss to the latter is often predominantly via optical phonons.[23] We shall see later than optical phonons make a significant contribution to the room temperature capture cross section in silicon and germanium. (4) At low temperatures, at large distances from the trap, electrons will only have enough energy to emit acoustical phonons. The enormous cross sections reported in the helium temperature range (see Fig. 1) must then be associated with acoustical phonons.

## Thomson Theory of Recombination

The theory proposed in this paper leads to results [see Eq. (2.7)] that bear a close resemblance to the Thomson[24,25] theory of recombination in gases. In the

[20] The author is indebted to Albert Rose and G. H. Wannier for illuminating discussions of this point. In particular see the discussion following the author's paper in reference 19.

[21] G. Bemski, Phys. Rev. **100**, 523 (1955). See also reference 15.

[22] Auger recombination is observed by Haynes and Hornbeck[12] with extremely low cross sections of order $10^{-39}$ and $10^{-41}$ times the concentration of majority carriers for electrons and holes, respectively. This low cross section is presumably caused by the Coulomb repulsion of the center for majority carriers. Conversely, Auger trapping of electrons by attractive donors is observed by Koenig[9] with the enormous cross section of about $10^{-24}\,n$, where $n$ is the number of electrons per cm$^3$. Koenig's data refer to electrons of 100°K with the lattice in the 4°–10°K range. This large cross section requires an electron-electron collision as the first step, followed by a cascading process in which energy is conveyed to the lattice. A *rough* estimate by the methods explained later in this paper yields

$$\sigma(E_0)\approx(2\pi^2/3)n(e^2/\kappa E_0)^3(e^2/kT)^2.$$

The insertion of $T=6$°K, $E_0=k(100$°K), and $\kappa=16$, the dielectric constant of Ge yields $\sigma\sim0.6\times10^{-24}\,n$ cm$^2$!

[23] E. Conwell, J. Phys. Chem. Solids **8**, 234 (1959); T. Morgan, J. Phys. Chem. Solids **8**, 245 (1959); and J. Yamashita, Phys. Rev. **111**, 1529 (1958).

[24] J. J. Thomson, Phil. Mag. **47**, 337 (1924).

[25] H. S. W. Massey and E. H. S. Burhop, *Electronic and Ionic Impact Phenomena* (Oxford University Press, New York, 1952), Chap. X.

gas discharge case, one also has a "three-body collision," with the third body—a neutral atom—carrying off the energy. Thomson reasoned that ions with kinetic energy greater than $(3/2)kT$ will lose energy on collision. Ions with lower kinetic energy will gain energy on collision. Thus within a critical radius $r_0$ defined by

$$Ze^2/r_0=(3/2)kT, \tag{1.7}$$

collisions will be effective in producing recombination, whereas outside this sphere they will produce separation. If $l$ is the mean free path for an energy losing collision, and $4r_0/3$ is the average distance across a sphere, $(4r_0/3l)$ is the probability of a suitable collision if one hits the sphere and $\pi r_0^2$ is the cross section for hitting the sphere. Thus Thomson proposed a cross section of the order

$$\sigma_{\text{Thomson}}\approx(4\pi/3)r_0^3/l. \tag{1.8}$$

The Thomson theory is implicitly predicated on the assumption that $r_0<l$ so that one or fewer collisions will occur, on the average, within the critical radius. In the opposite case, $r_0\gg l$, many collisions can occur within the critical radius. In this case, the reaction will be "diffusion limited" and the Langevin[25–27] theory is appropriate. The rate of influx through a sphere of radius $r$ per unit density of electrons is

$$B=4\pi r^2 v_d=4\pi r^2\mu(Ze/\kappa r^2), \tag{1.9}$$

or

$$B=4\pi Ze\mu/\kappa \text{ cm}^3/\text{sec},$$

where the drift velocity $v_d$ is calculated by multiplying the attractive field $Ze^2/\kappa r^2$ by the mobility $\mu$. In the gas discharge case, the Thomson theory predicts a recombination rate proportional to the pressure and is observed at low pressures, whereas the Langevin theory predicts a rate inversely proportional to the pressure and is observed at high pressures when the process becomes "diffusion limited."

The Langevin recombination rate can be converted to a cross section according to Eq. (1.5) by dividing by a thermal velocity. For electrons in silicon, the Langevin cross section at room temperature is about $10^{-9}$ cm$^2$ or at least four orders of magnitude larger than the largest observed cross sections. We may conclude that diffusion does not limit any of the electron trapping processes in solids.

To illustrate the Thomson approach, we shall apply his type of reasoning to make an estimate of the capture cross section associated with optical phonons of energy $\hbar\omega$. In order to emit such a phonon, electrons must have or acquire an energy $\hbar\omega$. They can certainly do the latter by coming within the critical radius $r_0=(Ze^2/\kappa\hbar\omega)$. Thus we may estimate the cross section to be

$$\sigma_{\text{opt}}\approx\frac{4}{3}\pi\left(\frac{Ze^2}{\kappa\hbar\omega}\right)^3\frac{1}{l_0}, \tag{1.10}$$

where the mean free path for $l_0$ *emission* of an optical phonon can be estimated from the "classical" mean free path $l_c$ for emission or absorption of acoustic phonons by

$$1/l_0=w(\hbar\omega/2kT)[1-\exp(-\hbar\omega/kT)]^{-1}(1/l_c), \tag{1.11}$$

where $w=(E_2/E_1)^2$ is the ratio of the squares of the interaction (or deformation) constants for the two types of modes; $1/l_c$ is proportional to the temperature and is defined by (1.22).

We shall see in Sec. 2 that the Thomson theory neglects a factor $E/E_0$ where $E_0$ is the initial energy of the electron and $E$ is the electron energy when the collision takes place. Thus our result [Eq. (1.10)] should be corrected roughly by a factor $\hbar\omega/kT$. Taking this correction into account $\sigma_{\text{opt}}$ behaves as $1/T$ when $kT\ll\hbar\omega$ and as independent of $T$ when $kT\gtrsim\hbar\omega$. When $kT\gg\hbar\omega$ Eq. (1.10) must be reduced by an appreciable probability of escape.

A similar qualitative analysis can be made for the case of acoustic phonons, but it must take proper account of the spectrum of possible energy losses. A careful qualitative estimate will therefore be as difficult as the more quantitative treatment presented later and we omit it here.

### Divergences

We may mention here that Wannier[28] has previously considered the interaction with acoustic phonons. He noted that electrons whose velocity $v$ is twice the velocity of sound $c$ can lose all their energy in a single collision with an acoustical phonon. Thus for these electrons the critical radius and the capture cross section are infinite. Wannier then suggested that observed lifetimes would be limited by the rate at which the supply of electrons of velocity $2c$ could be replenished. Such a rate would be independent of the number of traps present in contradiction with the experimental results for which the rate is proportional to the number of traps.

For optical phonons, a similar divergence occurs. Electrons of energy $E_0$ really have a critical radius $r_0=Ze^2/[\kappa(\hbar\omega-E_0)]$ since a gain in kinetic energy of $\hbar\omega-E_0$ is sufficient to permit radiation of a phonon of energy $\hbar\omega$. Thus as $E_0\rightarrow\hbar\omega$ a divergence occurs.

These divergences occur because the assumption has been made that any electron that goes into a bound orbit is eventually captured regardless of the size of the orbit. There are, obviously, some limits on the possible sizes of orbits: (1) the screening radius (for distances larger than the screening radius, there will be no po-

[26] P. Langevin, Ann. Chem. Phys. **28**, 289, 433 (1903).

[27] A generalization of the Langevin type theory to a case in which diffusion only partly limits the rate is given by S. I. Peckar, J. Exptl. Theoret. Phys. (U.S.S.R.) **20**, 267 (1950) [translation: Abhandlungen Soviet Phys. **1**, 47 (1951)]. For comments on this paper see reference 19.

[28] G. H. Wannier, Phys. Rev. **91**, 207(A) (1953).

tential to produce a bound orbit), (2) the average distance between traps (otherwise one assumes that a given center captures an electron that in reality is captured by another center), (3) the mean free path (at distances larger than the mean free path one should use a Langevin diffusion type of theory).

### Sticking Probability

In most experimental situations, however, we believe there is a more important limitation than those mentioned already. An electron captured into a state with binding energy $U$ small compared to $kT$ will find it easy to escape in a subsequent collision. If $P(U)$ is the "sticking probability" for a state of binding energy $U$, i.e., the probability that the electron will enter the ground state before escaping, then the cross section for capture of an electron of energy $E_0$ should be written

$$\sigma(E_0)=\int\sigma(E_0,U)dU\ P(U), \tag{1.12}$$

where $\sigma(E_0,U)dU$ is the cross section for capture into a state with binding energy between $U$ and $U+dU$.

To enter a state of binding energy $U$, the electron of energy $E_0$ must at least gain in kinetic energy an amount $U$, so that the critical radius is $(Ze^2/\kappa U)$, and Eq. (1.8) suggests that the cross section diverges[29] as $1/U^3$. The final result converges only because $P(U)$ vanishes sufficiently rapidly for small $U$.

In a fully quantum mechanical treatment Eq. (1.12) would be replaced by

$$\sigma(E_0)=\sum_{n,l}\sigma_{n,l}(E_0)P_{n,l}, \tag{1.13}$$

where $\sigma_{n,l}$ is the cross section for capture into a hydrogenic state with quantum numbers $n$ and $l$, and $P_{n,l}$ is the corresponding sticking probability. Our treatment, for simplicity, makes the approximation of neglecting the dependence of $P_{n,l}$ on $l$, i.e., on the angular momentum, and replaces the sum over $n$ by an integral over $U$. The last step should be a good approximation if the main contribution comes from excited states that are reasonably closely spaced.

The sticking probability $P(U)$ can be calculated by making use of the idea that it depends on the binding energy $U$ but not on how that state was reached. Thus if $K(U,\hbar\omega)d(\hbar\omega)$ is the probability that an electron in state $U$ will emit a phonon $\hbar\omega$ in $d(\hbar\omega)$, then

$$P(U)=\int_{U+\hbar\omega\geq 0}K(U,\hbar\omega)d(\hbar\omega)\ P(U+\hbar\omega) \tag{1.14}$$

represents the probability of entering the ground state as the probability of any first step times the probability that the first step leads to eventual capture in the ground state. Absorption of phonons is included in Eq. (1.14) by allowing $\hbar\omega$ to be negative. The lower limit expresses the assumption that once a state of negative binding energy (i.e., positive energy) is reached, the probability of capture into the ground state is negligible (the probability of any subsequent collision into any bound state is small if $r_0\ll l$).

The total probability of all possible steps out of $U$ is of course unity:

$$\int K(U,\hbar\omega)d(\hbar\omega)=1, \tag{1.15}$$

but the total probability within the range $U+\hbar\omega\geq 0$ is less than unity for those states $U$ from which escape is possible in a single collision. These assumptions about the kernel $K(U,\hbar\omega)$ are sufficient to ensure that $P(U)\equiv 1$ is not a solution and that not more than one solution of Eq. (1.14) exists. (A proof has been given by E. N. Gilbert of these laboratories.)

The virial theorem implies that an electron of binding energy $U$ has an average kinetic energy equal to $U$. Consistent with our neglect of the dependence of $P(U)$ on the angular momentum of the state, we shall neglect the fluctuations in kinetic energy over the orbit. Thus $K(U,\hbar\omega)$ can be obtained by calculating the (usual) rate at which free electrons of kinetic energy $U$, moving in a plane wave, have collisions with an energy loss $\hbar\omega$ and normalizing the result in accordance with Eq. (1.15).

If the total reciprocal mean free path $1/l(E)$ for electrons of energy $E$ is displayed as a sum of contributions with specific energy loss $\hbar\omega$,

$$1/l(E)=\int[1/l(E,\hbar\omega)]d(\hbar\omega), \tag{1.16}$$

then we shall refer to $1/l(E,\hbar\omega)$ as the differential reciprocal mean free path. Energy gains are covered by the case $\hbar\omega<0$. The appropriately normalized $K(U,\hbar\omega)$ can now be written in the form

$$K(U,\hbar\omega)=\frac{1/l(U,\hbar\omega)}{\int[1/l(U,\hbar\omega)]d(\hbar\omega)}. \tag{1.17}$$

For acoustic phonons, conservation of energy and momentum dictate that the integration range in Eqs. (1.16) and (1.17) be limited by

$$\hbar\omega/\tfrac{1}{2}mc^2\leq 4[(E/\tfrac{1}{2}mc^2)^{\frac{1}{2}}-1], \tag{1.18}$$

$$\hbar\omega/\tfrac{1}{2}mc^2\geq -4[(E/\tfrac{1}{2}mc^2)^{\frac{1}{2}}+1], \tag{1.19}$$

the maximum possible phonons that can be emitted, or absorbed, respectively, by an electron of energy $E$.

Within this range, the deformation potential theory, without neglect of phonon energy [see Appendix A, Eq. (A11)] indicates that for acoustic phonons the differential reciprocal mean free path has approximately

[29] Actually the probability of emission of a phonon varies as $(E-\hbar\omega)^{\frac{1}{2}}=(E_0+U-\hbar\omega)^{\frac{1}{2}}\approx U^{\frac{1}{2}}$ for $E_0\approx\hbar\omega$, so that the divergence is really $(1/U^{2.5})$.

the form

$$1/l(E,\hbar\omega)=B|\hbar\omega|(\hbar\omega/kT)\times[1-\exp(-\hbar\omega/kT)]^{-1}, \quad (1.20)$$

where $B$ cancels out of Eq. (1.17) but is given by

$$B=[8Emc^2l_c]^{-1}, \quad (1.21)$$

where $l_c$, the mean free path for electrons in the classical limit $kT\gg\hbar\omega$, is given by

$$1/l_c=E_1^2kTm^{\frac{3}{2}}/(\pi\hbar\rho c^2). \quad (1.22)$$

Here $c$ is the velocity of sound, $m$ is the effective mass of the electron, $\rho$ is the crystal density, and $E_1$ is the deformation potential constant. [In practice we shall determine $l_c$ from the experimental mobility rather than Eq. (1.22).]

Since electrons with a velocity less than that of sound can absorb phonons but cannot emit them, electrons with binding energy $U\leq\frac{1}{2}mc^2$ must eventually escape. Thus $P(U)=0$ for $U\leq\frac{1}{2}mc^2$, and the singularity[29] in $\sigma(E_0,U)\propto 1/U^{2.5}$ at $U=0$ will not cause a divergence. Even so, if $P(U)$ does not decrease rapidly as $U$ gets small (faster than $U^3$) it will turn out that the predominant contribution to the thermal average cross section will come from electrons of energy $E_0$ in the vicinity of $\frac{1}{2}mc^2$.

An analysis of the capture integral equation (1.14) by a Fokker-Planck type of diffusion approximation indicates that $P(U)$ varies as $U^3$ in the region $\frac{1}{2}mc^2\ll U\ll kT$. The contribution to the capture cross section by electrons of various energies then goes as $dE_0/(E_0)^2$. (See Sec. 5.) The low energy cutoff in $E_0$ must come then from an analysis of $P(U)$ in the low-energy region $U\gtrsim\frac{1}{2}mc^2$. In this "tail" region, however, the electron can escape in one jump, and the diffusion approximation is not valid.

To resolve these difficulties, the capture integral equation was solved by an iteration procedure using the diffusion solution as a first approximation. It was found that $P(U)$ does indeed decrease more rapidly than $(U-\frac{1}{2}mc^2)^3$ for $(U/\frac{1}{2}mc^2)<$about 4. In addition, it was found possible to simplify the integral equation in the tail region. When $\lambda\equiv(U/\frac{1}{2}mc^2)-1\ll 1$ it was possible to show that $P(U)\equiv P(\lambda)$ has an essential singularity near $\lambda=0$ of the form

$$P(\lambda)\propto\lambda^n,$$
$$n\approx 3.52+\ln(1/\lambda)/\ln 3+2\ln\ln(1/\lambda)/\ln 3+\cdots, \quad (1.23)$$

so that a more rapid vanishing than $\lambda^3$ is in general to be expected.

In using the concept of a sticking probability we have tacitly assumed that the diffusion up and down the energy scale occurs so rapidly that all time delays may be neglected. The electron is either captured into the ground state or escapes in a time small compared to the decay time in the experiment—otherwise non-exponential decays would be observed!

### Additional Simplifying Assumptions

In addition to our major assumptions concerning the use of classical mechanics and a sticking probability, depending only on binding energy, we shall make some nonessential but convenient assumptions: (1) the electrons motion is describable in terms of an isotropic effective mass (denoted simply by $m$). (2) The effects of transverse and longitudinal acoustic modes can be lumped together by using a single average velocity of sound and a single constant for the interaction of these modes with the electron. (3) Optical modes can be characterized by a single energy—the Einstein approximation.

The uncertainties introduced by these *additional* approximations, e.g., by our lack of knowledge of what to choose for the appropriate effective mass and interaction constant may easily cause an uncertainty of a factor of 2 or 3 but is unlikely to change the cross section by more than one order of magnitude.

## 2. QUANTITATIVE FORMULATION

In view of the large experimental cross section we conclude that the important contribution to capture comes from large orbits which may according to the Bohr correspondence principle[30] be treated classically. We shall therefore make an impact parameter calculation of the cross section

$$\sigma(E_0)=\int 2\pi b\,db\,P_c(E_0,b), \quad (2.1)$$

where $b$ is the impact parameter (see Fig. 2) and $P_c(E_0,b)$ is the probability that an electron with impact parameter $b$ and energy $E_0$ will somewhere along its orbit have an effective capturing collision. The above formulation emphasizes a single important collision and hence is a Thomson rather than Langevin approach to the problem.

The probability of capture along the orbit $P_c(E_0,b)$ can be written in the form[31]

$$P_c(E_0,b)=\int dt\int_{\hbar\omega\geq E_0} W[E(t),\hbar\omega]d(\hbar\omega)\times P(\hbar\omega-E_0), \quad (2.2)$$

where $W(E,\hbar\omega)d(\hbar\omega)$ is the transition probability per unit time for a collision with energy loss between $\hbar\omega$ and $\hbar\omega+d(\hbar\omega)$, $P(\hbar\omega-E_0)=P(U)$ is the sticking

[30] The classical viewpoint will be valid providing the important contributions come from distances large compared to the Bohr radius in the solid $\kappa\hbar^2/(Zme^2)$.

[31] Strictly speaking (2.2) is the expected number of capturing events along the orbit. For the case of Poisson statistics $\exp[-P_c(E_0,b)]$ is the probability of having no such collision, and $1-\exp[-P_c(E_0,b)]$ is the probability of capture along the orbit, which is of necessity less than unity. For the case in which $r_0\ll l$, considered here, $P_c\ll 1$, and the linear approximation $1-\exp(-P_c)\approx P_c$ is adequate.

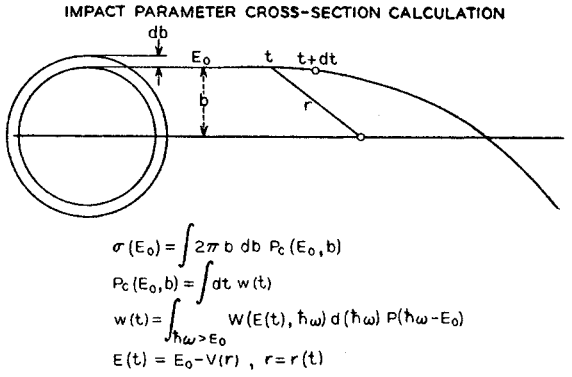


FIG. 2. The cross section is computed from the area struck (i.e., $2\pi b db$) times the probability $P_c(E_0,b)$ that a capture producing collision will occur somewhere along an orbit that starts with an energy $E_0$ and an impact parameter $b$. Here $w(t)$ is the probability per unit time of such a collision, when the electron has kinetic energy $E(t)$; $W(E(t),\hbar\omega)d(\hbar\omega)$ is the probability per unit time of a collision in which the energy $\hbar\omega$ is lost, $\hbar\omega-E_0$ is the resulting binding energy and $P(\hbar\omega-E_0)$ is the probability that an electron with this binding energy will "stick," i.e., enter the ground state before escaping.

probability for an electron with binding energy $U$ and

$$E(t)\equiv E_0-V[r(t)]=E_0+Ze^2/[\kappa r(t)] \qquad (2.3)$$

is the kinetic energy at the time $t$ on the orbit. The function $r(t)$ is to be obtained by solving the classical equation of motion for an electron with initial energy $E_0$, and impact parameter $b$.

It seems expedient to change the variable of integration from $t$ to $r$. The Jacobian of this transformation

$$dr/dt=(2/m)^{\frac{1}{2}}[E(r)-E_0(b^2/r^2)]^{\frac{1}{2}} \qquad (2.4)$$

is known from conservation of energy and angular momentum, without explicit need for the solution $r(t)$. If, in addition, we multiply and divide by $v=[2E(r)/m]^{\frac{1}{2}}$, (2.2) can be rewritten as

$$P_c(E_0,b)=2\int_{r_m} dr\frac{[E(r)]^{\frac{1}{2}}}{[E(r)-E_0(b^2/r^2)]^{\frac{1}{2}}} \times\int\frac{1}{v}W(E(r),E_0+U)dU\,P(U), \qquad (2.5)$$

where the factor 2 is inserted because the region from the minimum distance of approach $r_m$ to infinity is traversed twice—once inward, and once outward.

If (2.5) is inserted into (2.1) the integration over $b$ can be performed explicitly[32]:

$$\int_0^{b_M} bdb[E-E_0(b^2/r^2)]^{-\frac{1}{2}}=E^{-\frac{1}{2}}b_M{}^2 =r^2E^{\frac{1}{2}}/E_0, \qquad (2.6)$$

where $b_M=r(E/E_0)^{\frac{1}{2}}$ is the maximum impact parameter consistent with a given $r$. If the integration over $U$ is saved for last, the result may be written in the form (1.12) where the cross section $\sigma(E_0,U)dU$ for a collision into the binding energy $U$, $U+dU$ is given by

$$\sigma(E_0,U)=\int_0^{r_0}4\pi r^2dr[E(r)/E_0] \times[1/l(E(r),E_0+U)], \qquad (2.7)$$

where we have used the relation

$$1/l(E,\hbar\omega)=W(E,\hbar\omega)/v. \qquad (2.8)$$

The upper limit $r_0$ is the largest radius at which a collision with energy loss $E_0+U$ is possible.[33] Note the similarity of (2.7) to Thomson's original formula $4\pi r_0{}^3/3l'$ when $l'$ is some effective mean free path.

Equation (2.7) is general in that the mechanism of collision has not yet been specified: it may be, for example, collisions with lattice vibrations, or other carriers, in a solid, or collisions with neutral atoms in a gas. Furthermore, explicit use has not yet been made of the form of the potential $V(r)$. The only basic assumption has been the use of classical mechanics in the formulation of the capture cross section.

An acoustic phonon energy loss $E_0+U$, according to Eq. (1.18), requires an electron kinetic energy $E>E_m$ where

$$E_m=\tfrac{1}{2}mc^2[1+\tfrac{1}{4}(E_0+U)/\tfrac{1}{2}mc^2]^2. \qquad (2.9)$$

Thus the electrons must convert at least the energy $E_m-E_0$ from potential energy to kinetic energy, i.e., it must come within a radius $r_0$ determined by

$$-V(r_0)=E_m-E_0. \qquad (2.10)$$

For the Coulomb attractive case this yields

$$r_0=\frac{Ze^2}{\kappa}\frac{1}{\tfrac{1}{2}mc^2[1+\tfrac{1}{4}(E_0+U)/\tfrac{1}{2}mc^2]^2-E_0}, \qquad (2.11)$$

or

$$r_0\approx\frac{16Ze^2(\tfrac{1}{2}mc^2)}{\kappa(E_0+U)^2}. \qquad (2.12)$$

Equations (1.20) and (1.21) show that $E/l(E,\hbar\omega)$ is independent of $E$, so that the integration in Eq. (2.7) can be performed:

$$\sigma(E_0,U)=\frac{4\pi}{3}\frac{r_0{}^3}{E_0}\frac{(E_0+U)}{8mc^2l_c}\frac{\lambda}{1-\exp(-\lambda)}, \qquad (2.13)$$

where

$$\lambda=(E_0+U)/kT. \qquad (2.14)$$

Making use of Eq. (2.11) our differential cross

[32] If $b_M$ exceeds the screening radius, the distance between traps, or the mean free path, this upper limit must be modified.

[33] It should be remarked that if another cutoff $r_c$ is present—due to screening, or the distance between centers, etc.—then the upper limit of (2.7) should read $r_0$ or $r_c$ whichever is smaller. See also footnote 32.

section can be expressed in the form

$$E_0\sigma(E_0,U)=\sigma_1\frac{[(E_0+U)/\frac{1}{2}mc^2]^2}{\{[1+\frac{1}{4}(E_0+U)/\frac{1}{2}mc^2]^2-E_0/\frac{1}{2}mc^2\}^3}\times\frac{1}{1-\exp[-(E_0+U)/kT]}, \quad (2.15)$$

where

$$\sigma_1=\frac{\pi}{12}\left(\frac{Ze^2}{\kappa\frac{1}{2}mc^2}\right)^3\frac{1}{l_c}\frac{\frac{1}{2}mc^2}{kT} \quad (2.16)$$

is independent of temperature and has the units cm$^2$.

It is convenient to introduce the dimensionless variables:

$$\epsilon_0=E_0/\tfrac{1}{2}mc^2, \quad \eta=U/\tfrac{1}{2}mc^2, \quad \gamma=kT/\tfrac{1}{2}mc^2. \quad (2.17)$$

Then $\sigma(E_0,U)\equiv\sigma(\epsilon_0,\eta)$ can be obtained from

$$\epsilon_0\sigma(\epsilon_0,\eta)=\sigma_1\frac{(\epsilon_0+\eta)^2}{\{[1+\frac{1}{4}(\epsilon_0+\eta)]^2-\epsilon_0\}^3}\times\frac{1}{1-\exp[-(\epsilon_0+\eta)/\gamma]}. \quad (2.18)$$

If Eq. (2.18) is averaged over a Boltzmann distribution of electron fluxes, in the manner of Eq. (1.4) we obtain for the total cross section

$$\sigma=\int\sigma(\eta)d\eta\,P(\eta), \quad (2.19)$$

with

$$\sigma(\eta)=\int\epsilon_0\sigma(\epsilon_0,\eta)\exp(-\epsilon_0/\gamma)d\epsilon_0/\gamma^2$$

$$=\frac{\sigma_1}{\gamma^2}\int_0^\infty e^{-\epsilon_0/\gamma}d\epsilon_0\frac{(\epsilon_0+\eta)^2}{\{[1+\frac{1}{4}(\epsilon_0+\eta)]^2-\epsilon_0\}^3}\times\frac{1}{1-\exp[-(\epsilon_0+\eta)/\gamma]}. \quad (2.21)$$

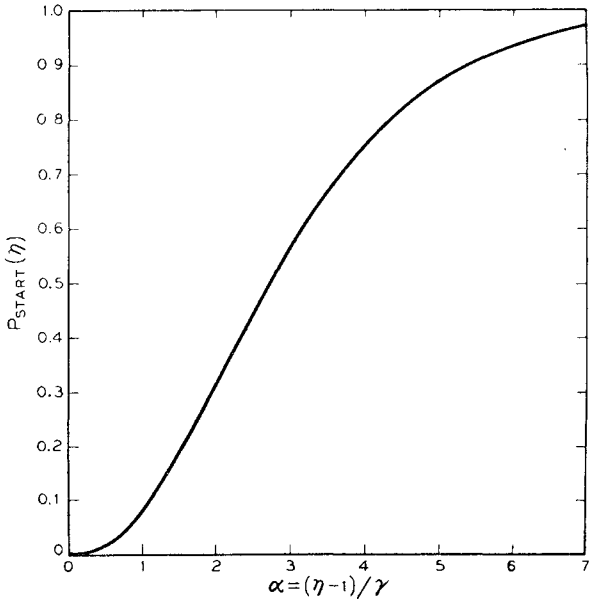


FIG. 3. A starting approximation $P_{\text{start}}$ for the sticking probability is plotted against $\alpha=(\eta-1)/\gamma$, where $\eta=U/\frac{1}{2}mc^2$, $\gamma=kT/\frac{1}{2}mc^2$, where $U$ is the binding energy, $T$ the absolute temperature, $m$ the carrier effective mass, and $c$ the velocity of sound. The starting approximation $P=1-(1+\alpha+\frac{1}{2}\alpha^2)\exp(-\alpha)$ is a simplification valid for $\gamma\gg1$ of the solution (B6) of the diffusion (Fokker-Planck) treatment of the sticking probability integral equation.

### 3. ESTIMATES OF THE TOTAL CROSS SECTION: COULOMBIC CENTERS, ACOUSTICAL PHONON CONTRIBUTION

The dominant behavior of $\sigma(\eta)$ as given by Eq. (2.21) is as $(\eta+4)^{-4}$ if $4\ll\eta\ll\gamma$. We therefore introduce into (2.21) the transformation

$$\epsilon_0=(\eta+4)x, \quad (3.1)$$

so that the dominant behavior is displayed in the form

$$\sigma(\eta)=\frac{4^6}{\gamma}\frac{\sigma_1}{(\eta+4)^4}h(\eta,\gamma), \quad (3.2)$$

where

$$h(\eta,\gamma)=\int_0^\infty g(x)dx, \quad (3.3)$$

$$g(x)=\exp\left[-\frac{\eta+4}{\gamma}x\right]\frac{\frac{\eta}{\gamma}+\frac{\eta+4}{\gamma}x}{1-\exp\left[-\left(\frac{\eta}{\gamma}+\frac{\eta+4}{\gamma}x\right)\right]}\times\frac{\frac{\eta}{\eta+4}+x}{\left[x^2+2\frac{\eta-4}{\eta+4}x+1\right]^3}. \quad (3.4)$$

We expect $h(\eta,\gamma)$ to be a slowly varying function. If $4\ll\eta\ll\gamma$, we see that

$$g(x)\approx(1+x)^{-5}; \quad h(\eta,\gamma)\approx\tfrac{1}{4}, \quad (3.5)$$

whereas if merely

$$\eta+4\ll\gamma,$$

$$g(x)\approx\left(\frac{\eta}{\eta+4}+x\right)\left[x^2+2\frac{\eta-4}{\eta+4}x+1\right]^{-3} \quad (3.6)$$

and

$$h(\eta,\gamma)\approx\tfrac{1}{4}+4^{-4}(\eta+4)^4\eta^{-2.5}I, \quad (3.7)$$

where

$$I=\int_a^\infty \frac{dy}{(1+y^2)^3}, \tag{3.8}$$

and

$$a=[(\eta/4)-1]\sqrt{\eta}.$$

The second term in Eq. (3.7) varies as $\eta^{-6}$ for large $\eta$ and is negligible compared to the first except for small $\eta$. (At $\eta=4$ the two terms are almost equal.) Near $\eta=0$, the second term diverges as $\eta^{-2.5}$. This is essentially the divergence found by Wannier, whose origin is discussed in the Introduction.[29] If one were to assume $P(\eta)=1$ as Wannier does (or even a small constant) the integral Eq. (2.19) for the total cross section would diverge. However, as we show in Appendix B, $P(\eta)$ varies faster than $(\eta-1)^3$, so that the second term in Eq. (3.7) has indeed little effect on the result.

If Eq. (2.19) is integrated by parts,

$$\sigma=\int_0^\infty \left[\int_\eta^\infty \sigma(\eta')d\eta'\right]\frac{dP}{d\eta}d\eta. \tag{3.9}$$

A rough approximation to the total cross section can be obtained assuming

$$\sigma(\eta)\approx(4^5\sigma_1/\gamma\eta^4), \tag{3.10}$$

and from Appendix B, or Figs. 3–5

$$\begin{aligned} dP/d\eta &\approx(\eta^2/2\gamma^3)\exp(-\eta/\gamma) \quad \text{for} \quad \eta>\delta \\ &\approx 0 \qquad\qquad\qquad\qquad \text{for} \quad \eta<\delta, \end{aligned} \tag{3.11}$$

where $\delta$ of 4 to 10 represents a cutoff in the region where $\sigma(\eta)$ begins to level off and $P(\eta)$ decreases more rapidly than (3.11a) indicates. These crude approximations lead to

$$\sigma\approx\frac{4^5\sigma_1}{6\gamma^4}\int_{\delta/\gamma}^\infty \frac{e^{-x}}{x}dx, \tag{3.12}$$

or

$$\sigma\approx\frac{4^5\sigma_1}{6\gamma^4}\left[\ln\left(\frac{\gamma}{1.781\delta}\right)+\frac{\delta}{\gamma}\right], \tag{3.13}$$

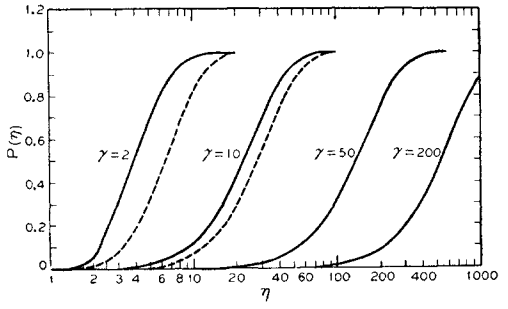


FIG. 4. Numerical solutions $P(\eta)$ of the sticking probability integral equation (B1) are plotted versus dimensionless temperatures $\gamma=kT/\frac{1}{2}mc^2=200$, 50, 10, and 2. These solutions were obtained by an iterative procedure using the starting approximation shown in Fig. 3. The dashed curves indicate the corresponding starting approximations. For $\gamma=50$ and 200 the correct solution is indistinguishable from the starting approximation on the scale shown, but their ratio is shown in Fig. 5.

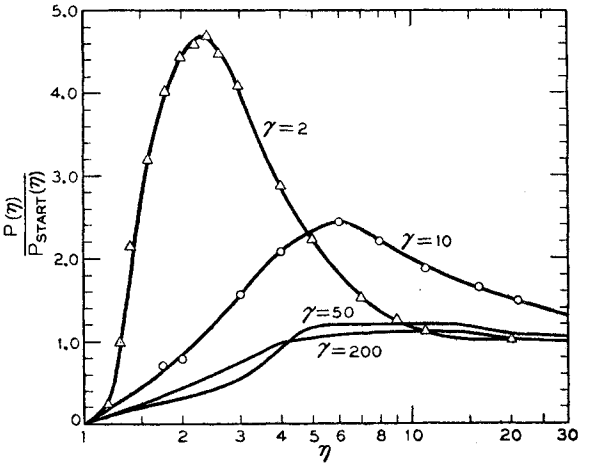


FIG. 5. The ratio of the sticking probability $P(\eta)$ to the starting approximation $P_{\text{start}}(\eta)$ of Fig. 3 is plotted against $\eta=U/\frac{1}{2}mc^2$.

where the last step replaces the exponential integral by an approximation valid when $\delta/\gamma<1$.

A more accurate evaluation of Eq. (3.3) for $h(\eta,\gamma)$ was made using the ten point Gauss-Laguerre quadrature formula[34] and the numerical capture probabilities $P(\eta)$, see Fig. 4, were obtained by numerical solution of Eq. (B1) for the cases $\gamma=2$, 10, 50 and 200 as discussed in Appendix B. The results obtained for $\sigma/\sigma_1$ are presented in Table II. A change of two orders of magnitude in $\gamma$ produces a change of 7 orders of magnitude in $\sigma/\sigma_1$. Column 3 of the table demonstrates that $\gamma^4\sigma/\sigma_1$ changes much more slowly.

In order to be able to interpolate or extrapolate from the four numerical results in Table II, it is desirable to have an even slower varying function than $\gamma^4\sigma/\sigma_1$. This desired property may be achieved by requiring the approximate formula (3.12) to agree with the machine results by allowing $\delta$ to be a function of $\gamma$. The values of $\delta$ needed to achieve agreement are shown in column 3 of Table II and do indeed vary slowly. A plot of $\delta$ versus $\gamma$ is shown in Fig. 6. Use of this figure to extrapolate to larger values of $\gamma$ is not risky since $\delta$ varies slowly and moreover according to Eq. (3.13) appears essentially as the argument of a logarithm.

TABLE II. Results of the machine computation for $\sigma/\sigma_1$ where

$$\sigma_1=\frac{\pi}{12}\frac{1}{l_c}\frac{Ze^2}{\kappa kT}\left(\frac{Ze^2}{\kappa\frac{1}{2}mc^2}\right)^2.$$

| $\gamma$ | $\sigma/\sigma_1$ | $(3/2)(\gamma/4)^4\sigma/\sigma_1$ | $\delta$ |
|---|---|---|---|
| 2 | $7.5\times10^{-1}$ | 0.070 | 3.5 |
| 10 | $1.03\times10^{-2}$ | 0.603 | 4.7 |
| 50 | $3.68\times10^{-5}$ | 1.35 | 8.6 |
| 200 | $2.62\times10^{-7}$ | 2.46 | 10.0 |

Here $\gamma=kT(\frac{1}{2}mc^2)$ and $\delta$ is computed from the second column by the requirement that the approximate formula Eq. (3.12) yield results in agreement with the machine calculation.

[34] H. E. Salzer and R. Zucker, Bull. Am. Math. Soc. **55**, 1004 (1949).

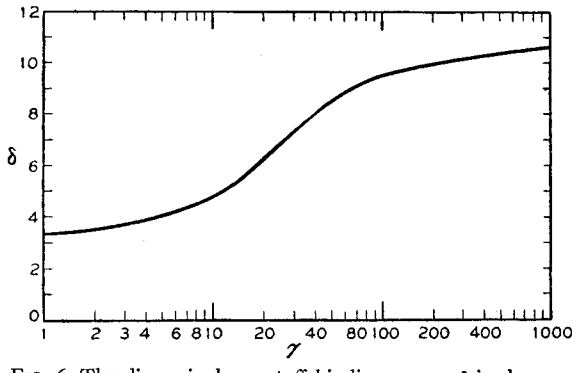


FIG. 6. The dimensionless cutoff binding energy $\delta$ is chosen as a function of dimensionless temperature $\gamma=kT/\frac{1}{2}mc^2$ so that the approximate equation (3.12) yields a cross section in agreement with that computed numerically for $\gamma=200$, 50, 10, and 2. This figure, by interpolation, permits the use of Eq. (3.12) to compute cross sections at other temperatures.

In order to compare our results with those of Koenig[9–11] for electrons captured by donors in germanium in the range of 9°K to 4°K we must choose an effective mass $m$, and a velocity of sound. Without a complete theory taking into account the mass anisotropy and the relative proportion of longitudinal and transverse phonon contribution to the capture all we can do is choose reasonable intermediate values, e.g., $m=\frac{1}{4}m_0$ and $c=4\times10^5$ cm/sec. Since the final results [Eq. (3.13)] indicate that the cross section is (aside from a logarithmic factor) proportional to $(mc^2)^2$ our results can easily be modified by a factor 3 by using other, equally reasonable values of $m$ and $c$. With these choices, $\frac{1}{2}mc^2=1.13\times10^{-5}$ ev $=0.131$°K and $e^2/(\frac{1}{2}\kappa mc^2)=7.9\times10^{-4}$ cm.

Another difficult thing to do accurately is to determine the mean free path $l_c$ for acoustic phonon scattering. Morin and Maita[35] have attempted to separate the acoustic phonon contribution. Their conclusion for the mobility in the presence of pure acoustic scattering is

$$\mu=2.4\times10^7T^{-1.5}, \tag{3.14}$$

with a room temperature mobility of 4600 cm²/volt sec. The mobility is related to the transport mean free time $\tau$ by

$$\mu=e\tau/m_I, \tag{3.15}$$

where the inertial mass $m_I$ is the harmonic mean of the parallel mass $m_{\parallel}=1.64$ and the two perpendicular masses $m_{\perp}=0.0819$, i.e., $m_I=0.12m_0$ where $m_0$ is the free electron mass. Thus the room temperature $\tau$ is $3.15\times10^{-13}$ sec, and the room temperature mean free path is

$$l_c=(9\pi kT/8m)^{\frac{1}{2}}\tau, \tag{3.16}$$

or $l_c\approx8.0\times10^{-6}$ cm if one uses $m=\frac{1}{4}m_0$. The room temperature value of $\gamma=kT/\frac{1}{2}mc^2$ is 2300. But the product $\gamma l_c=1.84\times10^{-2}$ cm is independent of temperature. The applicability of this result in the helium temperature region may be checked by noting that Eq. (3.14) yields a mobility of 4°K of $3\times10^6$ cm²/volt sec in agreement with the mobilities observed by Koenig[9–11] on his unusually pure sample in the He temperature range. We find then, that our temperature independent unit of cross section is given by

$$\sigma_1=Z^3(\pi/12)(e^2/\kappa\tfrac{1}{2}mc^2)^3(l_c\gamma)^{-1}\approx7\times10^{-9}Z^3 \text{ cm}^2. \tag{3.17}$$

With this unit of cross section (for $Z=1$), Eq. (3.13) and Fig. 6 as a means of interpolating $\delta$, cross sections were calculated in the range 4°K to 10°K. Our theoretical results and Koenig's experimental results[9–11] are shown for comparison in Fig. 1. Both experimental and theoretical results increase from $10^{-13}$ cm² to $10^{-12}$ cm² in the range from 10° to 4°K, with the experimental results increasing slightly less rapidly and showing definite signs of a level-off near 4°K. Confirmation of this level-off is shown in more recent data extended to lower temperatures. See Fig. 7.

For comparison, we note that the (acoustic phonon) theoretical cross section at room temperature $5.1\times10^{-19}$ cm² is so small as to be unimportant.

For silicon, we shall use $m=\frac{1}{2}m_0$, $\frac{1}{2}mc^2\approx10^{-4}$ ev and for electrons $l_c\approx3.2\times10^{-6}$ cm based on a room temperature mobility of 1200 and an inertial mass of $0.259m_0$. Thus we obtain as a unit of cross section $\sigma_1=5.45\times10^{-10}$ cm² for electrons in silicon. At room temperature $\gamma=260$ and Eq. (3.13) with $\delta\approx11.5$ yields $\sigma/\sigma_1\approx10^{-7}$ so that $\sigma\approx0.5\times10^{-16}$ cm². This cross section is about one order of magnitude lower than Bemski's reported cross section for electrons on $Au^+$ of $3.5\times10^{-15}$ cm². However, Bemski's cross sections in the range 200° to 500° show a $T^{-2.5}$ behavior rather than a $T^{-4}$ behavior. We believe this is due to an appreciable contribution from intervalley collisions and optical phonon collisions whose contribution will be estimated shortly.

For holes in silicon, the mobility is about one-fifth that of electrons. Other things being approximately equal, this leads to a cross section five times larger or $2.5\times10^{-16}$ cm² at room temperature, a result that is still low compared to Bemski's value (Table I) of $1\times10^{-15}$ cm² for holes on $Au^-$. Optical phonon contributions are also to be expected for holes in silicon since the hole mobility[36] varies as $T^{-2.3}$ deviating from the ideal acoustic law of $T^{-1.5}$.

## 4. OPTICAL AND INTERVALLEY PHONON CONTRIBUTION: COULOMBIC CENTERS

For optical and intervalley phonons we may take (see Appendix A) the differential reciprocal mean free path to have the form

$$\frac{1}{l(E,E_0+U)}=\frac{w}{2l_c}\frac{\lambda}{1-\exp(-\lambda)}\frac{(E-\hbar\omega)^{\frac{1}{2}}}{E^{\frac{1}{2}}}\times\delta(\hbar\omega-E_0-U), \tag{4.1}$$

[35] F. Morin and J. P. Maita, Phys. Rev. **94**, 1525 (1954).

[36] F. J. Morin and J. P. Maita, Phys. Rev. **96**, 28 (1954).

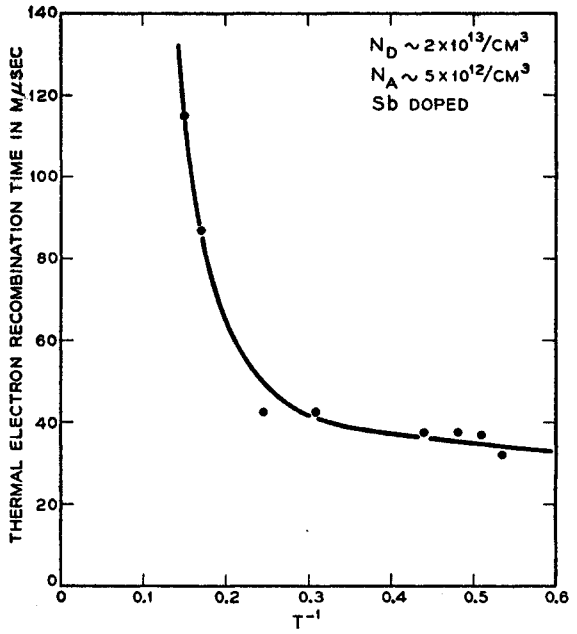


FIG. 7. Recombination of electrons on Sb donors in Ge at low temperatures by S. Koenig. The measurements shown in Fig. 1 have been extended to lower temperatures and continue to display the level off in the cross section which starts at about 4°K.

where $\hbar\omega$ is the single phonon energy, $\lambda=\hbar\omega/kT$ and $w$ is Herring's[37] factor describing the squared ratio of optical to acoustical matrix elements. The assumption that optical or intervalley phonons can each be represented by a single phonon energy is certainly accurate enough for our purposes.

If Eq. (4.1) and Eq. (2.7) are inserted into Eq. (1.12) the integration over $U$ can be performed immediately with the result

$$E_0\sigma_{\rm opt}(E_0)=2\pi(w/l_c)\lambda[1-\exp(-\lambda)]^{-1}\times P(\hbar\omega-E_0)J, \quad (4.2)$$

where

$$J=\int_0^{r_0} r^2dr[E(E-\hbar\omega)]^{\frac{1}{2}}, \quad (4.3)$$

$$E=E_0-V(r), \quad (4.4)$$

and the upper limit $r_0$ occurs when $E=\hbar\omega$. For the case of a Coulomb potential $V(r)=-Ze^2/kr$, we may use (4.4) to introduce $E$ as a new variable of integration:

$$J=\left(\frac{Ze^2}{\kappa}\right)^3\int_{\hbar\omega}^{\infty}\frac{dE}{(E-E_0)^4}[E(E-\hbar\omega)]^{\frac{1}{2}}. \quad (4.5)$$

The transformation $E-E_0=(\hbar\omega-E_0)(1+y)$ leads to

$$J=\left(\frac{Ze^2}{\kappa}\right)^3\frac{(\hbar\omega)^{\frac{1}{2}}}{(\hbar\omega-E_0)^{\frac{5}{2}}}\int_0^{\infty}\frac{dy}{(1+y)^4}y^{\frac{1}{2}}(1+ay)^{\frac{1}{2}}, \quad (4.6)$$

where $a=(\hbar\omega-E_0)/\hbar\omega<1$.

[37] C. Herring, Bell System Tech. J. 34, 237 (1955).

The integral in Eq. (4.6) may be evaluated by using a mean value $y=\bar{y}$ in the factor $(1+ay)^{\frac{1}{2}}$. The optical phonon cross section (3.35) then becomes

$$E_0\sigma_{\rm opt}(E_0)=\frac{\pi^2}{8}\frac{w}{l_c}\frac{Ze^2}{\kappa}\left(\frac{Ze^2}{\kappa\hbar\omega}\right)^2\frac{\lambda}{1-\exp(-\lambda)}\times\frac{P(\hbar\omega-E_0)}{[1-(E_0/\hbar\omega)]^{\frac{5}{2}}}(1+a\bar{y})^{\frac{1}{2}}. \quad (4.7)$$

The mean value appropriate to the case $a\ll1$ is $\bar{y}=1$, and the mean value appropriate to the case $a=1$ obeys $(1+\bar{y})^{\frac{1}{2}}=(64/15\pi)$ or $\bar{y}\approx0.85$. However, when $a\ll1$, it does not matter what we put for $\bar{y}$, so that we shall incur a small final error by setting $\bar{y}\approx0.85$.

The cross section (4.7) for capture via optical phonons averaged over electron energies in accord with Eq. (1.4) becomes

$$\sigma_{\rm opt}(T)=\frac{\pi^2}{8}\frac{w}{l_c}\frac{Ze^2}{\kappa kT}\left(\frac{Ze^2}{\kappa\hbar\omega}\right)^2\frac{\lambda}{1-\exp(-\lambda)}C(\lambda), \quad (4.8)$$

$$C(\lambda)=\int_0^{\lambda}P(\lambda-x)e^{-x}[1-(x/\lambda)]^{-\frac{5}{2}}dx\times[1+\bar{y}-\bar{y}(x/\lambda)]^{\frac{1}{2}}, \quad (4.9)$$

where

$$P(y)\approx1-(1+y+\tfrac{1}{2}y^2)\exp(-y) \quad (4.10)$$

is the sticking probability[38] expressed in dimensionless units $y=U/kT$, and $\lambda=\hbar\omega/kT$. Since $x/\lambda\leq1$, and the integrand weights small values of $x/\lambda$, a maximum error of 35% and usually a much smaller error will be incurred if $[1+\bar{y}-\bar{y}(x/\lambda)]^{\frac{1}{2}}$ is approximated by $(1+\bar{y})^{\frac{1}{2}}\approx64/15\pi$. Thus we may write

$$\sigma_{\rm opt}(T)=\sigma_0\lambda[1-\exp(-\lambda)]^{-1}D(\lambda), \quad (4.11)$$

where

$$\sigma_0=\frac{8\pi}{15}\frac{wZ^3}{l_c}\frac{e^2}{\kappa kT}\left(\frac{e^2}{\kappa\hbar\omega}\right)^2 \quad (4.12)$$

is a unit of cross section independent of temperature, and

$$D(\lambda)=\int_0^{\lambda}P(\lambda-x)[1-(x/\lambda)]^{-\frac{5}{2}}\exp(-x)dx, \quad (4.13)$$

$$D(\lambda)=\lambda^{\frac{5}{2}}e^{-\lambda}\int_0^{\lambda}y^{-\frac{5}{2}}P(y)e^{y}dy. \quad (4.14)$$

By expanding the integrand of Eq. (4.14) in powers of $y$, we obtain an expansion convenient for small values

[38] This sticking probability is obtained in Appendix B by assuming that bound electrons "diffuse" up and down in energy by absorbing or emitting acoustic phonons. Optical phonons can, and should, be included in this diffusion process. This would require the solution of a new integral equation in Appendix B. The additional labor does not seem warranted in view of the fact that the general character of $P(U)$ will not change, i.e., $P(U)$ is small for $U<kT$ and approaches unity when $U\gg kT$.

of $\lambda$ but convergent for all values of $\lambda$:

$$D(\lambda)=\frac{\lambda^4}{9}e^{-\lambda}\left[1+\frac{3}{5}\frac{1}{4}\lambda+\frac{3}{7}\frac{1}{4\cdot5}\lambda^2+\frac{3}{9}\frac{1}{4\cdot5\cdot6}\lambda^3+\cdots\right]. \quad (4.15)$$

By expanding $[1-(x/\lambda)]^{-\frac{5}{2}}$ in powers of $x$ and using the relations

$$\int_0^\lambda f(y)(\lambda-y)dy=\int_0^\lambda dy_2\int_0^{y_2} f(y_1)dy_1, \quad (4.16)$$

$$\int_0^\lambda f(y)\frac{(\lambda-y)^n}{n!}dy=\int_0^\lambda dy_{n+1}\int_0^{y_{n+1}} dy_n\cdots \times\int_0^{y_2} dy_1 f(y_1), \quad (4.17)$$

we obtain the expansion

$$D(\lambda)=\pi_4(\lambda)\left[1+\frac{5}{2}\frac{1}{\lambda}\frac{\pi_5}{\pi_4}+\frac{5}{2}\frac{7}{2}\frac{1}{\lambda^2}\frac{\pi_6}{\pi_4}+\frac{5}{2}\frac{7}{2}\frac{9}{2}\frac{1}{\lambda^3}\frac{\pi_7}{\pi_4}+\cdots\right], \quad (4.18)$$

convenient at large $\lambda$ but convergent for small $\lambda$. The functions $\pi_\nu=\pi_\nu(\lambda)$ are defined by

$$\pi_\nu(\lambda)=e^{-\lambda}\sum_{j=\nu}^{\infty}\frac{\lambda^j}{j!}=1-e^{-\lambda}\sum_{j=0}^{\nu-1}\frac{\lambda^j}{j!}. \quad (4.19)$$

These functions are cumulative Poisson distributions and are tabulated by Fry.[39] The ratio $D(\lambda)/\pi_4(\lambda)$ is a slowly varying monotonically decreasing function with the value 8/3 at $\lambda=0$ and 1 at $\lambda=\infty$. A calculation of $D/\pi_4$ for a few values of $\lambda$ yields Fig. 8 which can be conveniently used for interpolation. Figure 8 and Fry's table of $\pi_4$ permits a ready evaluation of $D(\lambda)$ and the complete temperature dependence

$$\lambda[1-\exp(-\lambda)]^{-1}D(\lambda)$$

which are both shown in Fig. 9. We see that $D(\lambda)$ varies as $\lambda^4$ for small $\lambda$ (i.e., $T^{-4}$ for large $T$) and approaches unity for large $\lambda$ or small $T$. The complete temperature dependence varies then from $T^{-4}$ for $kT>\hbar\omega$ to $T^{-1}$ in the region $\hbar\omega\gg kT$ with an exponent of about 2.5 in the region $\hbar\omega\approx 4kT$.

A rough estimate of the size of the cross section in silicon can be obtained by evaluating the temperature independent unit of cross section $\sigma_0$ given by Eq. (4.12).

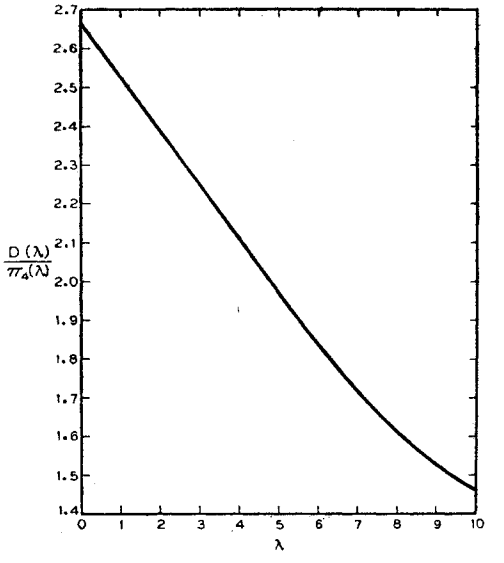


FIG. 8. A plot of $D(\lambda)/\pi_4(\lambda)$ versus $\lambda$ where

$$\pi_4(\lambda)=1-(1+\lambda+\tfrac{1}{2}\lambda^2+\tfrac{1}{6}\lambda^3)e^{-\lambda},$$

where $\lambda=\hbar\omega/kT$, and $D(\lambda)$ enters into the equation (4.11) for the cross section for capture by emission, of an optical phonon of energy $\hbar\omega$:

$$\sigma_{\rm opt}=\sigma_0[1-\exp(-\lambda)]^{-1}D(\lambda),$$

where

$$\sigma_0=\frac{8\pi}{15}\frac{wZ^3}{l_c}\frac{e^2}{\kappa kT}\left(\frac{e^2}{\kappa\hbar\omega}\right)^2,$$

$Z$=the charge on the trap, $\kappa$=dielectric constant, $l_c$=mean free path for an acoustical phonon collision, and $w$=squared ratio of optical to acoustical matrix elements.

Using $l_c\approx 320$ A for electrons, we find that

$$\sigma_{0,\text{ electrons in Si}}\approx 3.5\times10^{-15}wZ^3(0.1\text{ ev}/\hbar\omega)^2. \quad (4.20)$$

If we use as $\hbar\omega\approx 0.06$ ev for the optical phonons,[40] we get $\sigma_0\approx 10^{-14}w$ cm$^2$ for a singly changed center. At room temperature, however, $\lambda=\hbar\omega/kT\approx 2.4$ and, according to Fig. 9, the temperature dependent correction factor $\lambda[1-e^{-\lambda}]^{-1}D(\lambda)$ is about 1.5, so that the final estimated cross section $\sigma_{\rm opt}\approx wZ^3 1.5\times10^{-14}$ cm$^2$ is larger than the $3.5\times10^{-15}$ cm$^2$ observed by Bemski for electrons in $Au^+$ if we assume that the coupling constant ratio has a reasonable value $w\geq 1$ from the point of view of mobility.[36]

For holes in silicon, whose mean free path for acoustic scattering is perhaps five times smaller than for electrons, we find $\sigma_{\rm opt}\approx wZ^3 7.5\times10^{-14}$ cm$^2$ which appears five times larger then the just quoted cross section for electrons. However $w$ for holes is undoubtedly smaller than for electrons since the hole mobility varies as $T^{-2.3}$ whereas the electron mobility varies as $T^{-2.8}$.

For the first time in the history of calculating capture cross sections we are in the embarassing position of having theoretical answers larger than those observed

[39] T. C. Fry, *Probability and its Engineering Uses* (D. Van Nostrand Company, Inc., Princeton, New Jersey, 1928), Table VII, p. 463. See p. 336 for definition of symbols.

[40] B. N. Brockhouse, Phys. Rev. Letters **2**, 256 (1959). H. Palevsky, D. J. Hughes, W. Kley, and E. Tunkelo, Phys. Rev. Letters **2**, 258 (1959).

experimentally. There are two possible reasons for our overestimate:

(1) For $\lambda \geq 3$, we see that $D(\lambda) \approx 1$, i.e., we have effectively used sticking probabilities of unity. Our sticking probability was computed using an integral equation that involved emission and absorption of acoustic phonons only.[38] If we were to take into account optical phonons, then the sticking probability would be raised for binding energies large enough ($U \geq \hbar\omega$) to permit optical phonon emission. For lower binding energies, only optical phonon absorption is possible, and the latter will raise the probability of escape.

(2) In silicon $e^2/\kappa$ (0.06 ev) $\approx 20$ A is comparable to the Bohr radius of a donor state. Thus a strictly classical calculation will be somewhat of an overestimate since it includes some transitions to binding energies larger than the ground-state binding energy.

Another mechanism that may be of importance for electrons in silicon is intervalley scattering via an Umklapp process. The electronic band edge points in silicon are on the 100 axes about 85% of the way to the zone boundary.[41] Thus a transition to the ellipse just across the zone boundary can be accomplished via an Umklapp process using a phonon[40] about 30% of the maximum longitudinal acoustic phonon or about 0.019 ev. Thus $\sigma_0 \approx 10^{-13} w Z^3$, $\lambda \approx 0.73$ and

$$\lambda[1-\exp(-\lambda)]^{-1} D(\lambda)$$

is about 0.024, so that $\sigma_{\text{intervalley}} \approx 2.4 w Z^3 \times 10^{-15}$ cm$^2$. This process involves larger orbits, is less subject to quantum mechanical corrections, and is in rough agreement with Bemski's room temperature cross section of $3.5 \times 10^{-15}$ cm$^2$.

## 5. DEPENDENCE OF THE ACOUSTIC PHONON CROSS SECTION OF ELECTRON ENERGY

The dependence of the cross section on electron energy is shown explicitly in Eq. (4.7) for the optical phonon case. For the acoustic phonon case, we may start with Eq. (2.15) for $\sigma(E_0,U)$ and integrate over $U$. In the physically important case $kT \gg \frac{1}{2}mc^2$ we may approximate Eq. (2.15) by

$$E_0\sigma(E_0,U) \approx \frac{4^6 \sigma_1 [\frac{1}{2}mc^2/(E_0+U)]^4}{1-\exp[-(E_0+U)/kT]}. \quad (5.1)$$

If we substitute Eq. (5.1) into Eq. (1.12) and introduce the dimensionless variables

$$x = E_0/kT, \quad y = U/kT, \quad \gamma = kT/\tfrac{1}{2}mc^2, \quad (5.2)$$

then the dependence $\sigma(x)$ of the cross section on dimensionless energy $x$ is determined by

$$x\sigma(x) = (4^6/6)(\sigma_1/\gamma^4) F(x), \quad (5.3)$$

[41] G. Feher, J. Phys. Chem. Solids 8, 486 (1959).

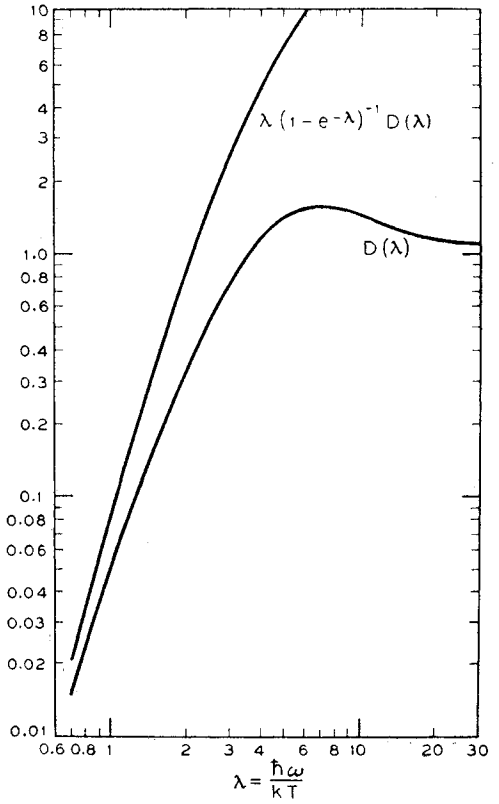


FIG. 9. A plot of $D(\lambda)$ and $\lambda[1-\exp(-\lambda)]^{-1}D(\lambda)$ versus $\lambda = \hbar\omega/kT$. The cross section for capture via optical phonons is given by $\sigma = \sigma_0\lambda[1-\exp(-\lambda)]^{-1}D(\lambda)$ where $\sigma_0$ is a unit of cross section independent of temperature given in Fig. 8 and Eq. (4.12). $\sigma$ varies as $T^{-4}$ for $\lambda \ll 1$, and as $T^{-1}$ for $\lambda \gg 1$.

where

$$F(x) = 6\int_0^\infty \frac{P(y)/(x+y)^4}{1-\exp[-(x+y)]}\,dy, \quad (5.4)$$

and $P(y)$, the sticking probability, is given by Eq. (4.10), except in the region $y \leq \delta/\gamma$ where a cutoff is more appropriate [see Eq. (3.11)]. If the cutoff is neglected, Eq. (5.4) yields

$$F(x) \approx \frac{1}{4x} - \frac{1}{4}\ln\left(\frac{1}{1.781x}\right) + O(x\ln x) \quad x \ll 1, \quad (5.5)$$

$$F(x) \approx \frac{2}{(x+6)^3}\,\frac{\exp[9/(x+3)]}{1-\exp(-x)} \quad x \gg 1. \quad (5.6)$$

Numerical results for $F(x)$ in the range $1/16 \leq x \leq 4$, obtained by numerical integration are shown in Fig. 10. Outside this range Eqs. (5.5) and (5.6) are good to within a few percent.

Equation (5.5) implies that $x\sigma(x) \sim 1/x$ for small $x$ so that the total cross section

$$\sigma = \int x\sigma(x)\exp(-x)dx, \quad (5.7)$$

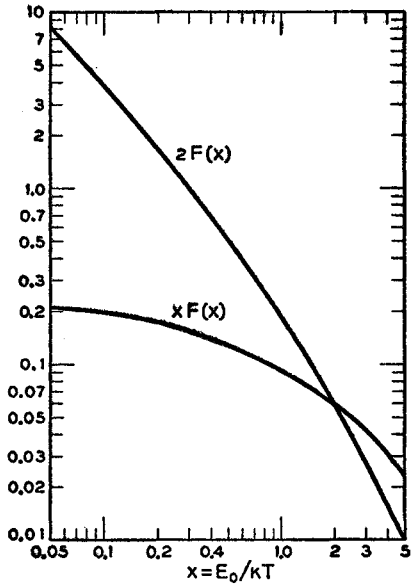


FIG. 10. The theoretical dependence of the cross section on electron energy $E_0$ is represented in the form

$$\sigma(x)=(4^6/6)(\sigma_1/\gamma^4)F(x)/x,$$

where

$$x=E_0/kT,\quad \gamma=kT/(\tfrac{1}{2}mc^2).$$

$T$ is the lattice temperature and $\sigma_1$ is a unit of cross section defined by Eq. (2.16). In the region $0.1<x<1$, $\sigma(x)\propto x^{-2.3}$.

would diverge at $x=0$. However, the cutoff in $dP/dy$ for $y\leq\delta/\gamma$ used in Eq. (3.11) implies that for $x\ll1$, the behavior $1/(4x)$ is to be replaced roughly by

$$F(x)\approx(\tfrac{1}{4})[x+(\delta/\gamma)]^{-1}, \tag{5.8}$$

so that Eq. (5.8) is convergent and yields approximately the answer (3.12) obtained when the integrations over $E_0$ and $U$ were performed in the opposite order.

The first term of (5.5) implies that over the range of importance $F(x)\propto 1/x$ and $\sigma(x)\propto 1/x^2$, i.e., $\sigma(E_0)\propto(1/E_0)^2$. Experimental decay times for a monoenergetic electron beam should then vary as $[(E_0)^{\frac{1}{2}}\sigma(E_0)]^{-1}$ or $E_0^{1.5}$.

Actually as Fig. 10 shows $xF(x)$ is not constant but varies as roughly $(1/x)^{0.3}$ over the range $1/16<x<1$. This would raise all exponents by 0.3. This small modification, however, is largely cancelled, if one takes account of the fact that one has a distribution of electron energies. For example, if the electrons have a temperature $T_e\neq T$, Eq. (1.4) with the modified distribution yields

$$\sigma(T,T_e)=(T/T_e)^2\int x\sigma(x)\exp[-Tx/T_e]dx. \tag{5.9}$$

The first factor indicates a behavior $1/T_e^2$ in agreement with the previous result $1/E_0^2$, and the integral is practically independent of $T_e$ since it can be evaluated approximately by replacing the exponential by unity.

Koenig's (reference 11) experimental decay times, shown in Fig. 11 vary with the effective electron temperature as $(T_e)^{1.8}$ corresponding to a cross section $\sigma$ which varies as $(T_e)^{-2.3}$.

## 6. TRAPPING BY NEUTRAL IMPURITIES

### Polarization Potential

A charge $e$ at a distance $r$ from a center with polarizability $\alpha$ will induce a moment $p=\alpha e/(\kappa r^2)$, where $\kappa$ is the dielectric constant of the medium. This dipole will produce an attractive force on the charge of $2pe/(\kappa r^3)=2\alpha e^2/(\kappa^2 r^5)$, so that an attractive potential exists of amount

$$V(r)=-A/r^4, \tag{6.1}$$

$$A=\tfrac{1}{2}\alpha e^2/\kappa^2. \tag{6.2}$$

The usual formula for the polarizability of an atom applies to our case

$$\alpha=(e^2h^2/4\pi^2m)\textstyle\sum_n f_n/(h\nu_n)^2, \tag{6.3}$$

where $h\nu_n$ is the energy difference between the ground state and state $n$, and $f_n$ is the corresponding oscillator strength. For an extended center, the electronic mass

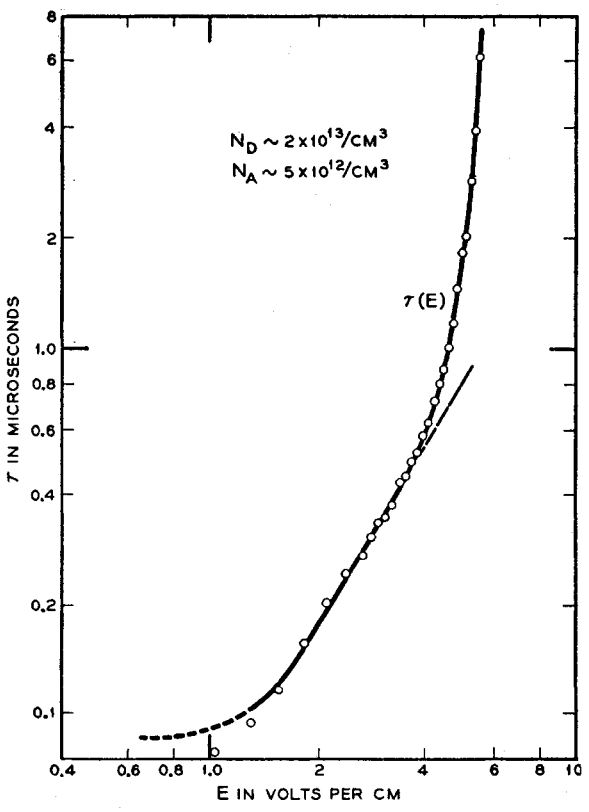


FIG. 11. The dependence on electric field of the lifetime for thermal recombination of electrons with Sb donors in Ge as measured by S. Koenig. In the straight line region the "hot" electrons have an energy approximately proportional to the field, so that the recombination time varies roughly as (electron energy)$^{1.8}$.

$m_0$ is replaced by the effective mass $m$. (For a highly localized electron it is more proper to use the ordinary mass $m_0$.) Since $\sum f_n=1$ a rough estimate can be made from (6.3):

$$\alpha\approx(e^2\hbar^2)/(4\pi^2mI^2), \tag{6.4}$$

or

$$\alpha/\alpha_H\approx(m_0/m)(I_H/I)^2, \tag{6.5}$$

where $I$ is the ionization energy of the center, $I_H=13.6$ ev is ionization energy of a hydrogen atom, and

$$\alpha_H=(9/2)(a_H)^3=0.666\times10^{-24}\text{ cm}^3 \tag{6.6}$$

is the polarizability of a hydrogen atom.[42] We see that large polarizabilities may be expected in solids because $I\ll I_H$ and $m<m_0$. In order to have a typical number in mind, we shall suppose that $I\lesssim0.5$ ev and $m\approx m_0$ for a moderately localized electron so that $\alpha$ by Eq. (6.5) is $\gtrsim4\times10^{-22}$ cm$^3$. (We assume that $I$ may be taken to be $\leq$ half the energy gap since a neutral center can be regarded as a charged center that has trapped an electron or a hole, and the smaller of the two ionization energies will determine the polarizability.)

For silicon, with $\kappa=12$, Eq. (6.2) yields $A=2\times10^{-31}$ ev cm$^4\approx20$ ev (A)$^4$. Of course, different centers in the same or different host lattices will have different polarizabilities. All we hope to do here is indicate the order of magnitude or the results, and many crude approximations will have to be made. For one, the potential $A/r^4$ must be cut off at some radius $R$. We shall assume that the potential is flat with the value $A/R^4$ for $0\leq r\leq R$, see Fig. 12, and shall choose $R$ small enough so that the second electron, the one to be captured, will have a binding energy $I$ in the WKB approximation. This leads to the condition[43]

$$\left[2m\left(\frac{A}{R^4}-I\right)\right]^{\frac{1}{2}}\int_0^R dr + \int_R^{r_1}\left[2m\left(\frac{A}{r^4}-I\right)\right]^{\frac{1}{2}}dr=\pi\hbar, \tag{6.7}$$

where

$$r_1=(A/I)^{\frac{1}{4}}.$$

In terms of the dimensionless variable

$$X_1=r_1/R=[A/(IR^4)]^{\frac{1}{4}}. \tag{6.8}$$

Equation (6.7) can be rewritten

$$X_1[1-(X_1)^{-4}]^{\frac{1}{2}}+F(X_1)=\pi[\hbar/(2mI)^{\frac{1}{2}}](I/A)^{\frac{1}{4}}, \tag{6.9}$$

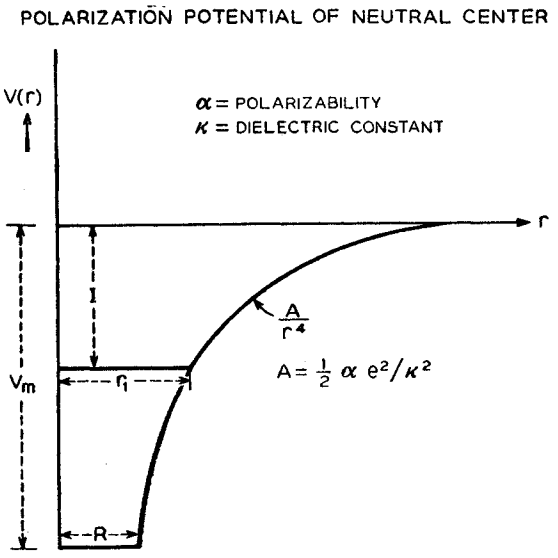


FIG. 12. The attractive potential exerted by the polarizability of an atom on a charge carrier has the form $V(r)=-A/r^4$ for $r\geq R$. We assume $V(r)=-A/R^4$ for $r\leq R$. The radius $r_1$ is defined by $V(r_1)=I=$ionization energy. The cutoff radius $R$ is chosen to be enough smaller than $r_1$ to produce a state with binding energy $I$.

where

$$F(X_1)=\left(1-\frac{1}{X_1^4}\right)^{\frac{1}{2}}X_1-1.20 + \frac{1}{2}\int_0^{(X_1)^{-4}} y^{-\frac{1}{4}}(1-y)^{-\frac{1}{2}}dy \tag{6.10}$$

is obtained from the second term in (6.7) by means of the transformation $r=r_1y^{\frac{1}{4}}$ followed by an integration by parts and 1.20 is an approximate value for $\Gamma(3/4)\Gamma(1/2)/\Gamma(5/4)$. Since $X_1>1$, $F(X_1)$ can be adequately approximated by

$$F(X_1)\approx X_1-1.20-1/(3X_1^3)+O[(X_1)^{-7}]. \tag{6.11}$$

If we choose $I\approx0.5$ ev for the ionization energy (of the second electron) and $A\approx20$ ev (A)$^4$ the right hand of Eq. (6.9) is approximately $\pi$, the solution for $X_1$ is 2.16 and $R$ using Eq. (6.8) is 1.16 A. This rather small value for $R$ is obtained because a fairly strong potential is needed to give the extra electron a 0.5-ev binding energy. The potential in the flat region is

$$V_m=A/R^4, \tag{6.12}$$

or approximately 11 ev.

### Optical Phonon Contribution to Neutral Capture

Equations (4.2) to (4.4) remain valid for the neutral case with $V(r)$ replaced by $-A/r^4$. Equation (4.3) for $J$ can be written

$$J=J_1+J_2, \tag{6.13}$$

[42] H. A. Bethe and E. E. Salpeter, *Quantum Mechanics of One- and Two-Electron Atoms* (Academic Press, Inc., New York, 1957), Sec. 52, Eq. (52.3) with $m=0$, $n_1-n_2=0$, $n=1$.

[43] The usual one-dimensional WKB method between two turning points would have $(n+\frac{1}{2})\pi\hbar$ on the right-hand side of Eq. (6.7). For a radial function, finite at the origin, the correct WKB condition leads to $(n+\frac{3}{4})\pi\hbar$. However, the correct answer is obtained in the hydrogenic case if one uses $(n+1)\pi\hbar$, or $\pi\hbar$ for the ground state, so we make the latter choice in (6.7).

where the contribution for the region where the potential is flat is

$$J_1=[E(E-\hbar\omega)]^{\frac{1}{2}}\int_0^R r^2dr \tag{6.14}$$

$$=[(E_0+V_m)(V_m-\hbar\omega+E_0)]^{\frac{1}{2}}R^3/3, \tag{6.15}$$

or

$$J_1\approx V_mR^3/3=A/(3R),$$

since $V_m=A/R^4\approx 11$ volts is large compared to $\hbar\omega$ and $E_0$. The portion of $J$ associated with the inverse $r^4$ region can be rewritten using $E=E_0+(A/r^4)$ as variable of integration:

$$J_2=\tfrac{1}{4}A^{\frac{3}{4}}\int_{\hbar\omega}^{V_m+E_0}\frac{dE}{(E-E_0)^{7/4}}[E(E-\hbar\omega)]^{\frac{1}{2}}, \tag{6.16}$$

or, letting $E-\hbar\omega=V_mz$,

$$J_2=\tfrac{1}{4}A^{\frac{3}{4}}V_m^{\frac{1}{4}}\int_0^{1-b}\frac{dz}{(b+z)^{7/4}}(f+z)^{\frac{1}{2}}z^{\frac{1}{2}}, \tag{6.17}$$

where

$$f=\hbar\omega/V_m\ll 1 \quad\text{and}\quad b=(\hbar\omega-E_0)/V_m\ll 1.$$

A sufficiently accurate value obtained by setting $b=f=0$,

$$J_2\approx A^{\frac{3}{4}}V_m^{\frac{1}{4}}=A/R, \tag{6.18}$$

is three times as large as the contribution $J_1$ of the flat region. The combined value $J=4A/(3R)$ with Eq. (4.2) yields a cross section

$$E_0\sigma(E_0)=(8\pi/3)(w/l_c)(A/R)\lambda[1-\exp(-\lambda)]^{-1}\times P(\hbar\omega-E_0). \tag{6.19}$$

The cross section for a thermal distribution of electrons according to Eq. (1.4) is

$$\sigma=(8\pi/3)(w/l_c)[A/(kTR)]\lambda[1-\exp(-\lambda)]^{-1}\bar{P}, \tag{6.20}$$

where

$$\bar{P}=\int_0^\infty P(\hbar\omega-kTx)\exp(-x)dx. \tag{6.21}$$

The sticking probability $P(U)$ should be recomputed for an inverse $r^4$ potential. In such a potential, however, there are no stationary closed orbits. The electron spirals inward (at least until the flat portion is reached). Thus the sticking probability should be larger than the corresponding $P(U)$ in the Coulomb attractive case. We shall therefore assume that $P(U)\approx 1$ as long as $U/kT$ is not small compared to unity. As long as $\hbar\omega\gtrsim kT$ then, we can approximate $\bar{P}$ by unity. The temperature dependence in Eq. (6.20) now resides entirely in the factor $\lambda[1-\exp(-\lambda)]^{-1}$ namely $\sigma\sim$ constant for $\hbar\omega<kT$ and $\sigma\sim 1/T$ for $kT\ll\hbar\omega$. Using $l_c\approx 320$ A for electrons in Si, $A\approx 20$ ev (A)[4] and $R\approx 1.16$ A, we get

$$\sigma\approx w\lambda[1-\exp(-\lambda)]1.7\times 10^{-15}\text{ cm}^2, \tag{6.22}$$

in order of magnitude agreement with Bemski's observed cross section of $8\times 10^{-16}$ cm$^2$ for electrons on Au$^-$.

### Acoustic Phonon Contribution to Neutral Capture

If we combine Eqs. (1.12) and (2.7) and use Eq. (1.20) to specify $1/l(E,\hbar\omega)$, we find that the cross section $\sigma(E_0)$ for electrons of energy $E_0$ obeys

$$E_0\sigma(E_0)=\frac{4\pi}{8mc^2l_c}\int_0^{\hbar\omega_m}\frac{P(\hbar\omega-E_0)\lambda\,|\,\hbar\omega\,|\,d(\hbar\omega)}{[1-\exp(-\lambda)]}\times\int_0^{r_0}r^2dr, \tag{6.23}$$

where $\lambda=\hbar\omega/kT$ as usual. Since an electron of kinetic energy $E$ large compared to $\frac{1}{2}mc^2$ can according to Eq. (1.18) lose a maximum energy of $4(E\frac{1}{2}mc^2)^{\frac{1}{2}}$, the maximum acoustic phonon that can be emitted is roughly

$$\hbar\omega_m\approx 4(V_m\tfrac{1}{2}mc^2)^{\frac{1}{2}}, \tag{6.24}$$

where $V_m\approx A/R^4\approx 11$ ev is the maximum depth of the potential, so that $\hbar\omega_m\approx 0.13$ ev if we use $\frac{1}{2}mc^2=10^{-4}$ ev which is appropriate for silicon. Of course, we must replace $\hbar\omega_m$ by the highest available acoustic frequency of roughly 0.049 ev. Conversely, in order to be able to emit a phonon of energy $\hbar\omega$ the electron must come within a radius of roughly

$$r_0\approx 2(A/\tfrac{1}{2}mc^2)^{\frac{1}{4}}(\tfrac{1}{2}mc^2/\hbar\omega)^{\frac{1}{2}}. \tag{6.25}$$

Combining Eqs. (6.23), (6.24), and (6.25) we find

$$\sigma(E_0)=\frac{2\pi}{3}\left[\frac{A}{\frac{1}{2}mc^2}\right]^{\frac{3}{4}}\frac{1}{l_c}\left[\frac{\frac{1}{2}mc^2}{kT}\right]^{\frac{1}{2}}\frac{kT}{E_0}\times\int_0^{\lambda_m}\frac{P(\lambda-x)\lambda^{\frac{1}{2}}d\lambda}{1-\exp(-\lambda)}, \tag{6.26}$$

where we have written $\lambda=\hbar\omega/kT$, $\lambda_m=\hbar\omega_m/kT$, $x=E_0/kT$; $P$ has been rewritten as a function of dimensionless variables and vanishes for $\lambda<x$. Since $\lambda_m>1$, one may approximate $P(\lambda-x)$ by unity and $\exp(-\lambda)$ by zero so that the integral in Eq. (6.26) is roughly $(2/3)(\lambda_m)^{\frac{3}{2}}$. Taking a thermal average by means of Eq. (1.4) we obtain

$$\sigma=\frac{2\pi}{3}\left(\frac{A}{\frac{1}{2}mc^2}\right)^{\frac{3}{4}}\frac{1}{l_c}\left(\frac{\frac{1}{2}mc^2}{kT}\right)^{\frac{1}{2}}\int_0^{\lambda_m}e^{-x}dx\times\int_0^{\lambda_m}\frac{P(\lambda-x)\lambda^{\frac{1}{2}}d\lambda}{1-\exp(-\lambda)}. \tag{6.27}$$

Making the approximation $P(\lambda-x)=1$, when $x<\lambda$ the double integral in Eq. (6.27) then reduces precisely to

$(2/3)(\lambda_m)^{\frac{3}{4}}$, so that

$$\sigma \approx \frac{4\pi}{9}\left(\frac{A}{\frac{1}{2}mc^2}\right)^{\frac{3}{4}} \frac{1}{l_c} \frac{[\frac{1}{2}mc^2(\hbar\omega_m)^3]^{\frac{1}{2}}}{(kT)^2}, \tag{6.28}$$

and the cross section varies as $1/T$. Inserting $A \approx 20$ ev (A)[4], $\frac{1}{2}mc^2 \approx 10^{-4}$ ev, $l_c \approx 320$ A, $\hbar\omega_m \approx 0.049$ ev, and $kT \approx 0.026$ ev we get a cross section at room temperature of roughly $6 \times 10^{-16}$ cm$^2$.

## 7. SUMMARY

In this paper we have explained giant trapping cross sections associated with Coulomb attractive centers by means of a large capture rate into highly excited states followed by a cascade process in which a certain fraction of the captured electrons reach the ground state. Acoustic and optical mode phonon creations provide the mechanism for energy loss.

Capture by neutral centers is treated in a similar way with the polarization of the neutral center providing excited states via an inverse fourth power potential.

A detailed summary of the results obtained here has been presented to the 1958 International Conference on Semiconductors and will not be repeated here. We only mention here that our theory for the acoustic phonon contribution predicts a cross section which increases rapidly as the temperature is lowered (because of effective capture into larger and larger orbits) in agreement with Koenig's experimental data (see Fig. 1). Koenig's cross section, however, starts to level off at 4°K (see Fig. 7) whereas ours continues to rise. We have previously suggested that this level-off must occur because at these temperatures contributions to the cross section comes from orbits comparable in size to the separation between the centers. Our computed levelled-off cross section, however, was too large to agree with Koenig's measurement.

Mattis[44] has recently suggested another reason for the observed cross section to level off. His reasoning is based on our result that the cross section varies approximately as $(1/E_0)^2$ for electrons of energy $E_0$ [see Eqs. (5.3)–(5.5) and Fig. 10]. Mattis suggested that in Koenig's experiment the large capture cross section for low-energy electrons depletes the supply of low-energy electrons so that the "average" cross section is reduced. Perhaps a combination of these explanations can yield quantitative agreement.

## 8. ACKNOWLEDGMENTS

It is a pleasure to acknowledge the assistance of Mrs. Gwen Hansen and Mrs. Lillian Lee with the analog and digital computations and to thank Dr. S. Koenig for making his data available to us before publication. The author is grateful to Dr. G. K. Wertheim for his invaluable help in constructing Table I.

[44] D. C. Mattis (private communication).

## APPENDIX A

### Collision Rates: Acoustic Phonons

The total rate of collisions of electrons with lattice vibrations can be written, using the deformation potential theory,[45] in the form

$$1/\tau(E) = \frac{E_1^2 kT}{4\pi^2\hbar^4\rho c^2} \int d\mathbf{p}' \frac{c^2|\mathbf{p}'-\mathbf{p}|^2}{(\hbar\omega)^2} M, \tag{A1}$$

where[46]

$$M = \tfrac{1}{2}\hbar\omega/kT[(\bar{n}+1)\delta(E(\mathbf{p}')-E(\mathbf{p})+\hbar\omega) + \bar{n}\delta(E(\mathbf{p}')-E(\mathbf{p})-\hbar\omega)], \tag{A2}$$

$$\bar{n} = [\exp(\hbar\omega/kT)-1]^{-1}, \tag{A3}$$

and $E_1$ is the deformation potential constant and $\rho$ the density of the crystal. We shall furthermore make the Debye approximation in which the phonon energy is given approximately by

$$\hbar\omega = c|\mathbf{p}'-\mathbf{p}|. \tag{A4}$$

For comparison, we note that in the usual ("classical") treatment of mobility, one makes the further assumption that $\hbar\omega \ll kT$ which is valid for the sort of collisions important in conductivity, but not for the collisions important in capture processes. In this "classical" approximation

$$M \approx \delta(E(\mathbf{p}')-E(\mathbf{p})), \tag{A5}$$

and

$$\int d\mathbf{p}'\delta(E'-E) = 4\sqrt{2}\pi m^{\frac{3}{2}}E^{\frac{1}{2}}. \tag{A6}$$

With these approximations, one obtains a "classical" mean free path approximately independent of electron energy:

$$\frac{1}{l_c} = \frac{1}{v\tau_c} = \frac{1}{\pi}\frac{E_1^2 kT m^{\frac{3}{2}}}{\hbar\rho c^2}, \tag{A7}$$

where $m$ is the effective mass in the crystal.

Comparing (A1) with the corresponding "classical" approximation we obtain

$$\frac{1/l(E)}{1/l_c} = \frac{\int d\mathbf{p}' M}{\int d\mathbf{p}'\delta(E'-E)}. \tag{A8}$$

The relation (A4) permits one to rewrite $d\mathbf{p}'$ as $dE'd(\hbar\omega)d\varphi$ where $\varphi$ is an azimuthal angle and $d\varphi$ may be replaced by $2\pi$:

$$d\mathbf{p}' = (2\pi m/pc^2)|\hbar\omega|d(\hbar\omega)dE'. \tag{A9}$$

[45] J. Bardeen and W. Shockley, Phys. Rev. 80, 72 (1950).

[46] The second term in the expression for $M$ (the absorption term) can be omitted if we allow $\omega$ in the first term to take negative values since $-\omega[\bar{n}(-\omega)+1] \equiv \omega\bar{n}(\omega)$.

If one uses (A6) for the denominator in (A8) and integrates over $E'$ in the numerator of (A8), the mean free path is given by

$$l_c/l(E)=(8Emc^2)^{-1}\int|\hbar\omega|d(\hbar\omega)\frac{\hbar\omega}{kT}\frac{1}{1-e^{-\hbar\omega/kT}}. \quad \text{(A10)}$$

Comparison of Eq. (1.16) with (A10) yields the reciprocal differential mean free path

$$1/l(E,\hbar\omega)=[|\hbar\omega|/(8Emc^2l_c)](\hbar\omega/kT)\times[1-\exp(-\hbar\omega/kT)]^{-1}. \quad \text{(A11)}$$

### Collision Rates: Optical and Intervalley

For optical and intervalley collisions we may regard the phonon energy $\hbar\omega$ as a constant, and modify the interaction $E_1^2$ by a factor $w$. Thus, if we rewrite (A2) as

$$M=\tfrac{1}{2}\lambda[1-\exp(-\lambda)]^{-1}\delta(E'-E+\hbar\omega), \quad \text{(A12)}$$

where

$$\lambda=\hbar\omega/kT, \quad \text{(A13)}$$

with absorption included when $\omega$ is negative then Eq. (A8) becomes

$$l_c/l(E)=w\int M d\mathbf{p}'\Big/\int\delta(E'-E)d\mathbf{p}'$$
$$=\tfrac{1}{2}w\lambda[1-\exp(-\lambda)]^{-1}[(E-\hbar\omega)/E]^{\frac{1}{2}}, \quad \text{(A14)}$$

and the reciprocal differential mean free path for energy loss $E_0+U$ can be written

$$\frac{1}{l(E,E_0+U)}=\frac{w}{2l_c}\frac{\lambda}{1-\exp(-\lambda)}\left(\frac{E-\hbar\omega}{E}\right)^{\frac{1}{2}}\times\delta(\hbar\omega-E_0-U). \quad \text{(A15)}$$

## APPENDIX B

### Sticking Probability Integral Equation

The integral equation (1.14) can be rewritten in terms of the dimensionless binding energy $\eta=U/(\frac{1}{2}mc^2)$ and the dimensionless energy loss $\mu=\hbar\omega/(\frac{1}{2}mc^2)$ in the form

$$P(\eta)=\int_{\eta+\mu\geq 1}K(\eta,\mu)d\mu P(\eta+\mu), \quad \text{(B1)}$$

where $K(\eta,\mu)$ is simply the differential reciprocal mean free path of Eq. (A11) normalized to unity:

$$K(\eta,\mu)=\frac{1}{N(\eta)}\frac{|\mu|\mu}{\gamma}\frac{1}{1-\exp(-\mu/\gamma)}, \quad \text{(B2)}$$

where $K(\eta,\mu)$ is understood to vanish outside the range of permissible energy losses and gains $-4(\sqrt{\eta+1})\leq\mu\leq 4(\sqrt{\eta}-1)$, and $N(\eta)$ is the normalizing factor

$$N(\eta)=\int_{-4(\sqrt{\eta+1})}^{4(\sqrt{\eta}-1)}\frac{|\mu|\mu}{\gamma[1-\exp(-\mu/\gamma)]}d\mu. \quad \text{(B3)}$$

The lower limit $\eta+\mu\geq 1$ is in accord with our discussion following Eq. (1.22) that $P(\eta)=0$ for $\eta\leq 1$.

### Diffusion Approximation

We note that for $\eta\gg 1$, the maximum energy loss $\mu\sim 4\sqrt{\eta}$ is small compared to $\eta$. It seems reasonable, then, to expand $P(\eta+\mu)$ in powers of $\mu$. The sticking probability Eq. (B1) then becomes

$$P(\eta)=\int_{\eta+\mu>1}K(\eta,\mu)d\mu P(\eta)+\int_{\eta+\mu>1}K(\eta,\mu)\mu d\mu P'(\eta)+\frac{1}{2}\int_{\eta+\mu>1}K(\eta,\mu)\mu^2P''(\eta)+\cdots. \quad \text{(B4)}$$

Such an expression is analogous to the Fokker-Planck treatment of the Brownian motion problem[47]: for sufficiently small steps an integral equation is replaced by a differential (diffusion) equation.

The first integral in Eq. (B4) represents the probability that after one collision the new binding energy $\eta'=\eta+\mu\geq 1$, i.e., the integral in question is the probability of not escaping on the first collision. For $\eta\geq 25$ the maximum energy gain $4(\sqrt{\eta+1})$ is insufficient to produce escape in one collision. Only in the region $\eta\gg 25$ will the energy gain or loss be small compared to $\eta$. Thus the integral equation itself *must* be used to investigate the tail region $\eta<25$, whereas the diffusion equation (B4) has some validity for $\eta\gg 25$. In the latter region, the requirement $\mu>-(\eta-1)$ can be dropped since $\mu>-4(\sqrt{\eta+1})$ is more stringent. Thus Eq. (B4) can be rewritten approximately as

$$P''(\eta)/P'(\eta)=d\ln P'(\eta)/d\eta=-2\langle\mu\rangle/\langle\mu^2\rangle=-f(\eta), \quad \text{(B5)}$$

where

$$\langle\mu^s\rangle=\int K(\eta,\mu)\mu^s d\mu$$

is the normalized $s$th moment of $\mu$. In other words, $\langle\mu\rangle$ is the mean energy loss and $\langle\mu^2\rangle$ is the root mean squared energy loss. The general solution to (B5) is

$$P(\eta)=1-A\int_\eta^\infty d\eta\exp\left[-\int^\eta f(x)dx\right], \quad \text{(B6)}$$

where we have made use of the boundary condition $P(\infty)=1$. Strictly speaking the integration constant $A$ should be so chosen that $P(\eta)$ matches with a solution

[47] S. Chandrasekhar, Revs. Modern Phys. **15**, 1 (1943), chap. I, Sec. 5.

suitable for the tail region. Roughly, however, we may extend (B6) into the tail region, and determine $A$ so that $P(1)=0$.

It is clear that a necessary requirement for the existence of a solution is that the integral in Eq. (B6) converge at infinity. Such convergence is assumed if $\lim \eta f(\eta)>1$, i.e.,

$$\lim_{\eta\to\infty} 2\eta\langle\mu\rangle/\langle\mu^2\rangle>1. \tag{B7}$$

The moments $\langle\mu\rangle$ and $\langle\mu^2\rangle$ are expressed by (B5) and (B2) in terms of tabulated definite integrals. For very large $\eta$ these integrals yield the asymptotic values $\langle\mu\rangle\to 3\sqrt{\eta}$ and $\langle\mu^2\rangle\to 48\eta/5$ so that condition (B7) is easily satisfied, and a solution exists. We could, then, tabulate the function $f(\eta)$ using (B5) and $P(\eta)$ using (B6).

We did not follow the above course of action since we did not wish to expend this much labor to obtain a solution only of the diffusion approximation. Instead, we note, that the diffusion approximation is likely to be valid only if $\gamma\gg 1$ and $\eta\gg 1$. In addition, we note that in the important region $\eta\approx\gamma$, the energy loss $4\sqrt{\eta}\ll\gamma$. Neglecting terms of order $1/\gamma$, $1/\eta$, and $4\sqrt{\eta}/\gamma$, we find that

$$\langle\mu\rangle\approx 8[(\eta/2\gamma)-1], \tag{B8}$$

$$\langle\mu^2\rangle\approx 8\eta, \tag{B9}$$

$$f(\eta)\approx(1/\gamma)-(2/\eta), \tag{B10}$$

$$dP(\eta)/d\eta\approx A\eta^2\exp(-\eta/\gamma) \tag{B11}$$

$$\approx A(\eta-1)^2\exp[-(\eta-1)/\gamma)]. \tag{B12}$$

Equation (B8) indicates that the mean energy loss $\langle\mu\rangle$ becomes positive at $\eta=2\gamma$ (or binding energies of 2 $kT$). From Eq. (B5), the zero of $\langle\mu\rangle$ at $\eta=2\gamma$ is also the point of inflection of $P(\eta)$. Thus the region in which $P(\eta)$ varies significantly is verified to be $\eta/\gamma\lesssim 1$, so that the approximations used in (B8)–(B10) are legitimate. Equation (B12) does not differ signicantly from Eq. (B11) within the approximation $1/\eta\ll 1$ but has the desirable property of vanishing at $\eta=1$. The integration of (B12) yields

$$P(\eta)\approx 1-\exp(-\alpha)[1+\alpha+\tfrac{1}{2}\alpha^2]\exp(-\alpha), \tag{B13}$$

where

$$\alpha=(\eta-1)/\gamma.$$

For small $\alpha$,

$$P(\eta)\approx\tfrac{1}{6}\alpha^3\approx(\eta-1)^3/6\gamma^3. \tag{B14}$$

A plot of (B13) is shown in Fig. 3. We shall refer to (B13) as the high-temperature diffusion approximation.

In the region in which $4\sqrt{\eta}/\gamma$ becomes comparable to unity, $P(\eta)$ will already be so close to unity that the neglect of $4\sqrt{\eta}/\gamma$ is unimportant.

Instead of attempting to improve the high-temperature diffusion result, we shall use Eq. (B13) as a starting approximation for the iterative solution of the original integral equation (B1). The Bell Laboratories analog computer was used to perform the iterations. Figure 5 shows that for $\gamma=200$ the high-temperature approximation is indistinguishable from the final correct result down to $\eta=20$ (the first iterate agreed with our trial function to within the accuracy 1% of the computer). A similar remark applies to $\gamma=50$ down to $\eta=40$. Note that $\gamma=200$ and 50 are roughly room temperature and liquid nitrogen temperature, respectively, for silicon. At lower temperatures ($\gamma=10$ and $\gamma=2$) the high-temperature approximation can no longer be expected to be valid, although it is qualitatively right. In Fig. 5 we see that the correct $P(\eta)$ in general exceeds the diffusion approximation, except at low binding energies ($\eta\lesssim 8$), because $P(\eta)$ vanishes much faster than $(\eta-1)^3$ as $\eta\to 1$. Qualitatively correct results can therefore be obtained by using the diffusion approximation Eq. (B13) cutoff at $\eta\approx\delta$ or with $\alpha$ replaced by $(\eta-\delta)/\gamma$ where $\delta$ is a number of the order 5 to 10. See Fig. 6.

### Tail Region

Since the total cross section might be significantly altered if $P(\eta)$ did not vanish as rapidly in the tail $\eta\ll 25$ as we claim, some detailed investigation of the tail region is in order. In the tail region $4\sqrt{\eta}\ll\gamma$, so that we may assume $\mu/\gamma\ll 1$ in the kernel (B2), with the result

$$K(\eta,\mu)\to[16(\eta+1)]^{-1}|\mu|. \tag{B15}$$

The kernel (B15) appropriate to the tail region is also the kernel of the infinite temperature ($\gamma=\infty$) case. With the latter viewpoint, we may consider $\eta>25$ as well as $\eta<25$.

Since $K(\eta,\mu,\gamma)$ becomes independent of $\gamma$ for small $\eta$, as in Eq. (B15), we may expect then, that the tails of the solutions for all $\gamma$ will be the same aside from a $\gamma$ dependent proportionality factor. This behavior is illustrated in Fig. 13. In that figure we see that the infinite temperature solution is the envelope of the solutions $\gamma^3P(\eta,\gamma)$.

If a Fokker-Planck expansion of the type (B4) is applied to the kernel (B15), one obtains a differential equation of the form

$$0=-2\left(\eta+\frac{1}{3}\right)P'+(\eta^2+6\eta+1)P''$$
$$-\frac{16}{15}(5\eta^2+10\eta+1)P^{(3)}-\frac{8}{9}(\eta^3+15\eta^2+15\eta+1)P^{(4)}$$
$$+O(\eta^3)P^{(5)}\cdots, \tag{B16}$$

in the region $\eta>25$. The first two terms in Eq. (B16) suggest that for large $\eta$ there is an approximate solution of the form $\eta^3$. Iteration, or the use of an assumed form

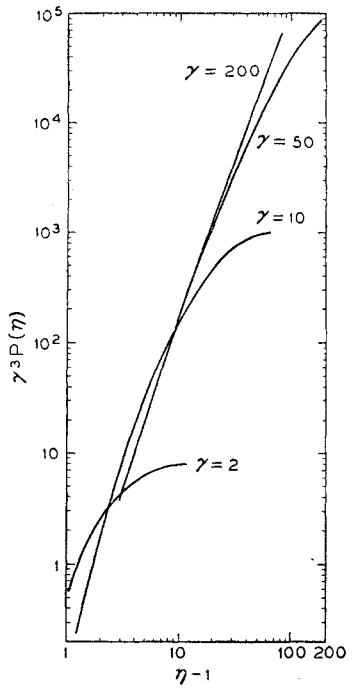


FIG. 13. A log-log plot of $\gamma^3 P(\eta,\gamma)$ versus $\eta-1$ where $\gamma=kT/\frac{1}{2}mc^2$ is a dimensionless temperature and $\eta=U/\frac{1}{2}mc^2$ is a dimensionless binding energy. The common envelope of these curves indicates that in the tail region $\eta \ll 25$, within one jump of the boundary, solutions at different temperatures are similar except for a temperature dependent normalization factor.

of solution leads to

$$P(\eta)=c\left[\eta^3+\eta^2-\frac{71}{3}\eta+\frac{128}{45}\ln\eta+\frac{128}{15}\frac{1}{\eta}+O\left(\frac{1}{\eta^2}\right)\cdots\right]. \quad \text{(B17)}$$

The higher order terms in Eq. (B16) are of the form $\eta^{n+1}P^{(2n)}$ and $\eta^{n+1}P^{(2n+1)}$. The introduction of higher order terms permits the determination of additional terms in Eq. (B17) without affecting the coefficients of the earlier terms. Thus a solution is uniquely determined.

It is clear that if we would impose the boundary conditions $P(\infty)=1$ on Eq. (B17) we would have $c=P(\eta)=0$, i.e., at infinite temperature the sticking probability at all binding energies is zero. For large but finite temperatures, there will be a region in which $25 \ll \eta \ll \gamma$. In this region, Eq. (B17), representing the high-energy end of the "tail solution" can be matched with the low-energy ($\eta/\gamma \ll 1$) end of the finite temperature solution. The latter is given roughly by Eq. (B14) so that we expect the constant $c$ to be of the form $(6\gamma^3)^{-1}$. Thus we expect that the functions $\gamma^3 P(\eta,\gamma)$ will coincide for sufficiently small $\eta$, with the infinite temperature solution providing an envelope (see Fig. 13).

Equation (B17), however, only represents an approximation, asymptotic for large $\eta$ to the infinite temperature solution. Equations (B17) and (B16) are both invalid at $\eta=25$ or even somewhat larger $\eta$ because

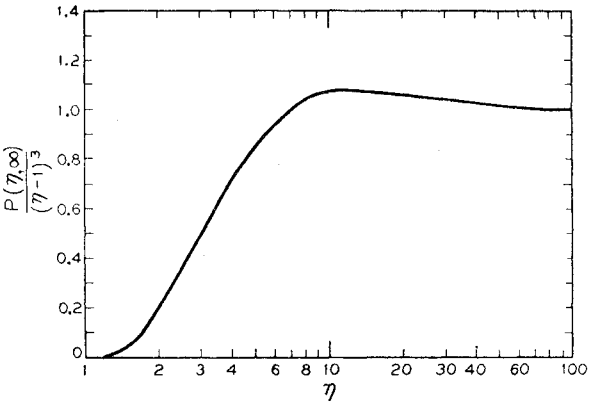


FIG. 14. The sticking probability $P(\eta)$ in the tail region divided by a starting approximation $(\eta-1)^3$ is plotted against $\eta$. $P(\eta)$ is obtained by numerical solution of Eq. (B1) using the kernel (B15) appropriate to the tail region, obtained by setting the temperature equal to infinity. The starting approximation is based on a Fokker-Planck treatment of the same equation.

$P''(\eta)$ has a discontinuity at $\eta=25$. This discontinuity arises because the lower limit to the integral equation (B1) changes from $\mu>-(\eta-1)$ to $\mu>-4(\sqrt{\eta}+1)$ at $\eta=25$. Equation (B17), therefore, may not be valid until $\eta$ is so big that only the $\eta^3$ term is of any consequence.

A reasonable procedure might be to use Eq. (B17) as a starting function in an iterative procedure. We shall see, however, that $P(\eta)$ vanishes quite rapidly as $\eta \to 1$. Therefore, a more suitable trial function over the whole range is

$$P_0(\eta) \approx (\eta-1)^3=\lambda^3. \quad \text{(B18)}$$

As evidence for the suitability of Eq. (B18) at large $\eta$ we note that if $P_1(\eta)$ is the first iterate, $P_1(100)/P_0(100)=1.0029$, so that Eq. (B18) is good to within a fraction of a percent at $\eta=100$, and better for larger $\eta$. Because of this success, we are able to assume (B18) to be valid for $\eta>100$, and to iterate below $\eta=100$. For practical purposes it is only possible to iterate over a finite region. Therefore it is necessary to have a solution good outside the finite region. And this is the reason we derive the asymptotic solution (B17). It is only by accident that the more convenient trial function $(\eta-1)^3$ is actually slightly better than the analytically obtained asymptotic solution (B17).

How good our trial function is may be seen by examining Fig. 14 which plots the ratio of $P(\eta)$ obtained after several iterations to $P_0(\eta)$. This ratio is close to unity in the region $\infty > \eta > 6$. For smaller values of $\eta$, $P/P_0$ decreases rapidly, reaching 0.5 near $\eta=3$ and 0 at $\eta=1$. Thus we find that in the region $\eta<6$, $P(\eta)$ decreases much more rapidly than $(\eta-1)^3$.

We now propose to explain the rapid decrease in $P(\lambda)$ as $\lambda=\eta-1$ approaches zero. [$P(\lambda)$ is simply $P(\eta)$ regarded as a function of $\lambda$.] The integral equation

(B17) using (B15) as kernel can be rewritten as

$$P(\lambda)=[16(2+\lambda)]^{-1}\int_a^{\lambda+4(1+\lambda)^{\frac{1}{2}}-4}|\lambda-\lambda'|\,d\lambda' P(\lambda'), \quad \text{(B19)}$$

where

$$a=0, \quad \text{for} \quad \lambda\leq 24$$
$$=\lambda-4(1+\lambda)^{\frac{1}{2}}-4 \quad \text{for} \quad \lambda\geq 24.$$

In the region $\lambda\ll 1$ Eq. (B19) reduces to

$$P(\lambda)=\frac{1}{32}\int_0^{3\lambda}|\lambda-\lambda'|\,d\lambda' P(\lambda'), \quad \text{(B20)}$$

a deceptively simple equation. To obtain the analytic dependence near $\lambda=0$, one might try $P(\lambda')=(\lambda')^n$. However, this yields $P(\lambda)\propto\lambda^{n+2}$, so that each iteration raises the exponent by two. Thus $P(\lambda)$ vanishes faster than $\lambda^n$ for any finite $n$. It is indeed not obvious, at all, that there is any analytic behavior near $\lambda=0$ that will satisfy Eq. (B20).

We can, however, obtain the nature of the singularity at $\lambda=0$ by a physical argument. Equation (B20) indicates that the probability of each (downward) step is of the order $\lambda$, so that $n$ downward steps occurs with a probability of the order $\lambda^n$. Since the binding energy can at most change from $\lambda$ to $3\lambda$, i.e., triple in each step, if $\lambda\ll 1$, the number of steps $n$ to go from $\lambda$ to a binding energy $b$ of order unity is given by

$$b/\lambda=3^n, \quad n=\ln_3(1/\lambda)+\ln_3 b, \quad \text{(B21)}$$

so that we expect

$$P(\lambda)\propto\lambda^n \quad \text{with} \quad n=\ln_3 b+\ln_3(1/\lambda),$$

as stated in Eq. (2.23) of the introduction.

The conjecture (B21) can be verified by converting Eq. (B20) to the differential difference equation

$$32P''(\lambda)=3P(3\lambda)+16\lambda P'(\lambda)+P(\lambda). \quad \text{(B22)}$$

A transformation to the new variables $\varphi(y)$ and $y$

$$P=e^{-\varphi} \quad \text{and} \quad \lambda=e^{-y}, \quad \text{(B23)}$$

permits (B22) to be rewritten after some rearrangement in the form

$$\varphi(y)-\varphi(y-\ln 3)=2y+\ln A, \quad \text{(B24)}$$

where

$$A=(32/3)[\varphi'+(\varphi')^2-\varphi'']+(16/3)\varphi' e^{-2y}-e^{-2y}. \quad \text{(B25)}$$

We are concerned with the solution of (B24) in the region of large $y$. The term in $2y$ is dominant, and may be used to obtain an approximate solution $\varphi\approx y^2/\ln 3$ that already contains the dominant behavior described in Eq. (1.23). One iteration using the dominant term in $A$, i.e., $A\approx(32/3)(\varphi')^2$ leads to

$$\varphi(y)\approx y^2/\ln 3+(2/\ln 3)y\ln y+cy+\cdots, \quad \text{(B26)}$$

where

$$c=\frac{1}{\ln 3}\left[\ln\left(\frac{128}{3(\ln 3)^2}\right)-2\right]\approx 3.52.$$

A return to the original variables gives $P\approx\lambda^n$ with

$$n\approx\ln(1/\lambda)/\ln 3+3.52+2\ln\ln(1/\lambda)/\ln 3. \quad \text{(B27)}$$

Equation (B27) verifies to good approximation our original conjecture Eq. (B21), and supplies us with an understanding of the nature of the essential singularity near $\lambda=0$.

PHYSICAL REVIEW VOLUME 119, NUMBER 5 SEPTEMBER 1, 1960

# Anisotropic Ferromagnetic Resonance Linewidth in Ferrites*

HERBERT B. CALLEN AND ERNEST PITTELLI
*Department of Physics, University of Pennsylvania, Philadelphia, Pennsylvania*

(Received April 28, 1960)

In disordered magnetic materials such as the ferrites, the dominant source of resonance linewidth can be attributed to processes involving only two elementary excitations: the destruction of a magnon with the creation either of another magnon or a phonon. We here consider only the primary magnon-magnon scattering process. We show that the random variation of the spin-orbit coupling parameters of the disordered ions leads to a resonance linewidth comparable to that observed in ferrites. The particular symmetry of the crystalline fields around the octahedrally coordinated sites causes an anisotropy in the linewidth with a minimum in the [100] directions and a maximum in the [111] directions. This anisotropy of linewidth is in general agreement with experimental observations on typical ferrites, as for example, the measurements of Schnitzler, Folen, and Rado on disordered lithium ferrite.

## 1. INTRODUCTION

THE source of resonance linewidth in disordered magnetic materials such as the ferrites has been discussed by Clogston, Suhl, Walker, and Anderson,[1] who pointed out the possibility of two excitation processes conserving energy but not momentum. The primary mechanism of magnon scattering was attributed to the random pseudodipolar interaction. However, the subsequent discovery by Folen and Rado[2] that the

* This work was supported by the Office of Naval Research.

[1] A. M. Clogston, H. Suhl, L. R. Walker, and P. W. Anderson, J. Phys. Chem. Solids **1**, 129 (1959).

[2] V. J. Folen and G. T. Rado, J. Appl. Phys. **29**, 438 (1958).